DAAD-19-99-1-0277

FINAL PROJECT REPORT

Experimental and Modeling Damage Limits Study for Straight Ti-3Al-2.5V Tubes

Team Members

Yaomin Lin, Kan Ni, Teh-Hwa Wong and Mool C. Gupta
University of Virginia

Kevin Woodland, Tim Grose, Tom Spidel, Bill Stone and Michael Yu
NAVAIR V-22 Program Office

Bob Taylor and Charles Lei
NAVAIR Materials

Reanne Williams
NAVAIR Hydraulics

Submitted to
Mr. Kevin Woodland
NAVAIR V-22 Program Office

Principal Investigator: Prof. Mool C. Gupta
Department of Electrical & Computer Engineering, University of Virginia,
Charlottesville, Virginia 22904
Email: mgupta@virginia.edu
Phone: 757-325-6850
Fax: 757-325-6988

May 15, 2007

Report Documentation Page

Form Approved
OMB No. 0704-0188

1. REPORT DATE	2. REPORT TYPE	3. DATES COVERED
27 AUG 2007		**15-09-2005 to 30-06-2007**

4. TITLE AND SUBTITLE	5a. CONTRACT NUMBER
Experimental and Modeling Damage Limits Study for Straight Ti-3A1-2.5V Tubes	5b. GRANT NUMBER
	5c. PROGRAM ELEMENT NUMBER
6. AUTHOR(S)	5d. PROJECT NUMBER
	5e. TASK NUMBER
	5f. WORK UNIT NUMBER
7. PERFORMING ORGANIZATION NAME(S) AND ADDRESS(ES) **University of Virginia,Office of Sponsored Programs,1001 N. Emmett St, P.O. Box 400195,Charlottesville,VA,22904-4195**	8. PERFORMING ORGANIZATION REPORT NUMBER
9. SPONSORING/MONITORING AGENCY NAME(S) AND ADDRESS(ES)	10. SPONSOR/MONITOR'S ACRONYM(S)
	11. SPONSOR/MONITOR'S REPORT NUMBER(S)

12. DISTRIBUTION/AVAILABILITY STATEMENT
Approved for public release; distribution unlimited

13. SUPPLEMENTARY NOTES
Government Purpose Rights

14. ABSTRACT

15. SUBJECT TERMS

16. SECURITY CLASSIFICATION OF:			17. LIMITATION OF ABSTRACT	18. NUMBER OF PAGES	19a. NAME OF RESPONSIBLE PERSON
a. REPORT	b. ABSTRACT	c. THIS PAGE			
unclassified	**unclassified**	**unclassified**	**Same as Report (SAR)**	**94**	

EXECUTIVE SUMMARY

To insure the safety of the V-22 aircraft over long period of operation, damage limits should be established for Ti alloy hydraulic tubes. In a previous report, the damage limit results for straight Ti-3Al-2.5V tubes with outer diameter (OD) of 3/8 inch and tube wall thickness of 0.032 inch were summarized. In this report, we present the fatigue life cycle (internal impulse pressure) test results and give the fatigue life trends for the straight Ti alloy tubes with ODs of ¼ inch, 3/8 inch, ½ inch, 5/8 inch and ¾ inch and the corresponding tube wall thicknesses of 0.022 inch, 0.032 inch, 0.043 inch, 0.054 inch and 0.065 inch, respectively. Presented results are worst case life cycles for short and long cracks or scratches based on sharp notch studies. Post-fracture crack profiling results for both short and long cracks are also presented. Finite element modeling was conducted for the prediction of the damage limits of various tubes and the results are compared with experiments with good agreement. Periodic inspection of Ti alloy tubes in combination with damage limit curves will provide a powerful tool to fleet maintainer for change of unsafe tubes. This was a successful collaborative effort between the researchers at the University of Virginia, V-22 program office, NAVAIR materials and hydraulics testing laboratories. Main conclusions of this study are: (1) the ¼ inch OD tube is the worst case; (2) cracks longer than 0.020 inch in length with nominal depth of 0.002 inch will have reduced life cycle than expected value of 200,000; (3) none of the tubes survived expected 200,000 fatigue cycles for long cracks.

Contents

ACKNOWLEDGMENT

This work was supported by NAVAIR under contract No. DAAD-19-99-1-0277 and administered by the Army Research Office. We also thank NSF I/UCRC program for their support. Our special thanks to Mr. Bill Stone for his vision and support.

1 Introduction

Ti-3Al-2.5V alloy has many superior properties such as high tensile strength, excellent resistance to torsion and corrosion, amenable to cold working, and weldability. Therefore, it is used principally as tubing in aircraft hydraulic systems. The reliability of the Ti-3Al-2.5V alloy tubing is adversely affected by damage in service. Ti-3Al-2.5V alloy tubing could fail prematurely under cyclic hydraulic pressurization. If the surface crack is initiated and developed through the tube wall, the hydraulic oil will leak out of the tubing, resulting in lower oil pressure, malfunction of hydraulic system, and also fire. As a result, it is very important to characterize the hydraulic impulse fatigue crack initiation and growth and correctly estimate the lives or damage limits of the Ti-3Al-2.5V tubes.

The focus of the "Damage Limits Study for Straight Ti-3Al-2.5V Tubes" project is to assure the safety of the aircraft and provide airframe maintainer and quality personnel tools to determine if the tube should be removed from the aircraft. By laboratory testing, finite element analysis and fracture mechanics study, damage limit curves of the titanium tubes have been developed and applied to determine the acceptable defect depth and length to avoid hydraulic leak failure within required service hours.

As an addition to the achievement made in the first phase of the project, where the damage limit curves of the straight tube with 3/8" outer diameter (OD) and 0.032" tube wall thickness (TWT) were studied, the impulse pressure test results for laser micromachining notched straight titanium tubes with ¼" OD × 0.022" TWT, ½" OD × 0.043" TWT, 5/8" OD × 0.054" TWT, and ¾" OD × 0.065" TWT, are summarized. The numerical modeling by means of finite element method and fracture mechanics method for the fatigue life prediction of the tubes are also described in this report.

2 General Conclusions

Based on the experimental and modeling study of the fatigue life of straight titanium alloy tube, the following major results and conclusions are drawn:

1. Observation of scratches and brass particles on inside surface of Ti tubing during bending process. This lead to change in process where plastic mandrel is used;
2. Experimentally, we have shown that laser micromachining provides sharp notch so that crack initiation life is small and can be neglected;
3. Generated experimental results for Ti tubing damage limits for short and long cracks, allowing the indication of the tube's service life;
4. Tubes can withstand over 200,000 pressure cycles (normal operational pressure) if notch length < 0.020" and depth <0.006";
5. For any specific notch depth, the longer the notch, the shorter the fatigue life. Above certain notch length, no significant difference in fatigue lives was observed;
6. For any specific notch length, the deeper the notch, the shorter the fatigue life of the tube;
7. Developed methodology and obtained modeling results for Ti tubing damage limits for short and long cracks;
8. Provided a methodology for long crack growth fatigue life determination that agrees with experiments;
9. Good agreement with experiment and modeling results were achieved;
10. 1/4" tube is the worst case from modeling and experimental results;

11. Developed an improved pre-notch fabrication process using laser micromachining method;
12. Developed an electrical potential method for crack growth measurements;
13. Long cracks (> 0.050”):
    1) For 1/4 inch tube size, life cycles is only ~80k cycles for 2 mil notch depth and will have even shorter life cycles for bent tubes;
    2) For 1/4 inch tube size, life cycle reduces to ~25k cycles for 4 mil notch depth and will have even shorter life for bent tubes.

As a result, significant attention needs to be paid to 1/4 inch tubes.

3 Comparison with Modeling and Experiments

Through experimental impulse pressure test, the fatigue lives of the laser micromachining notched straight titanium tubes with ¼” OD × 0.022” TWT, 3/8” OD × 0.032” TWT, ½” OD × 0.043” TWT, 5/8” OD × 0.054” TWT, and ¾” OD × 0.065” TWT, were determined. Numerical method of finite element modeling and fracture mechanics study were conducted and the prediction of the fatigue lives of those tubes was obtained.

Figure A shows the comparison of the finite element modeling and experimental data for the 1/4 inch OD tubes. It is seen that with a few exceptions, the modeling prediction data agrees well with the experiments. The comparisons of the modeling and experimental data for the 1/2 inch OD, 5/8 inch OD, 3/4 inch OD and 3/8 inch OD tubes are shown in Figures B-E, respectively.

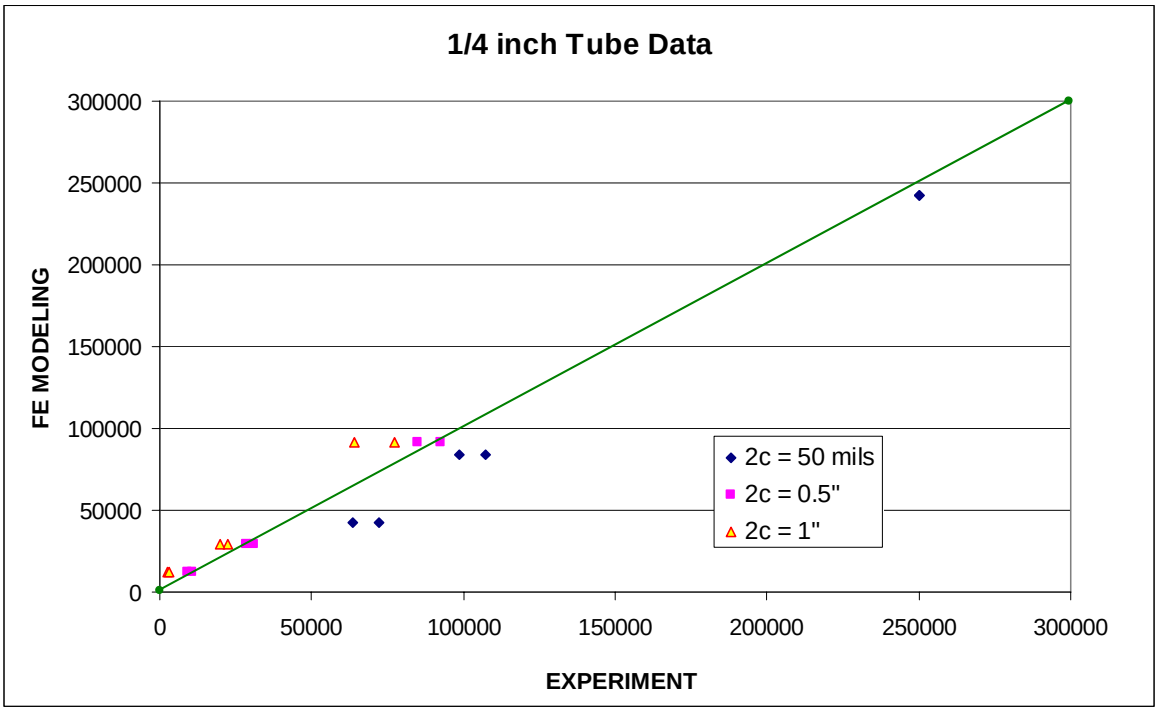

Figure A. Comparison of fatigue lives of 1/4 inch titanium tube between finite element modeling prediction and experiments.

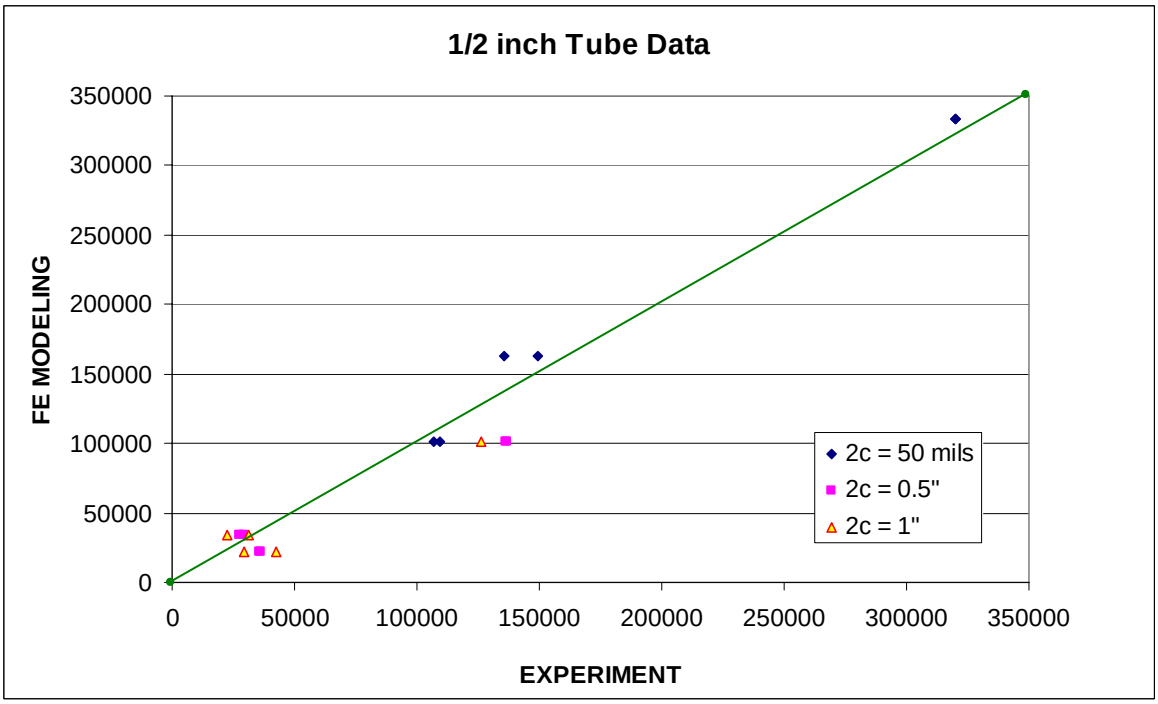

Figure B. Comparison of fatigue lives of 1/2 inch titanium tube between finite element modeling prediction and experiments.

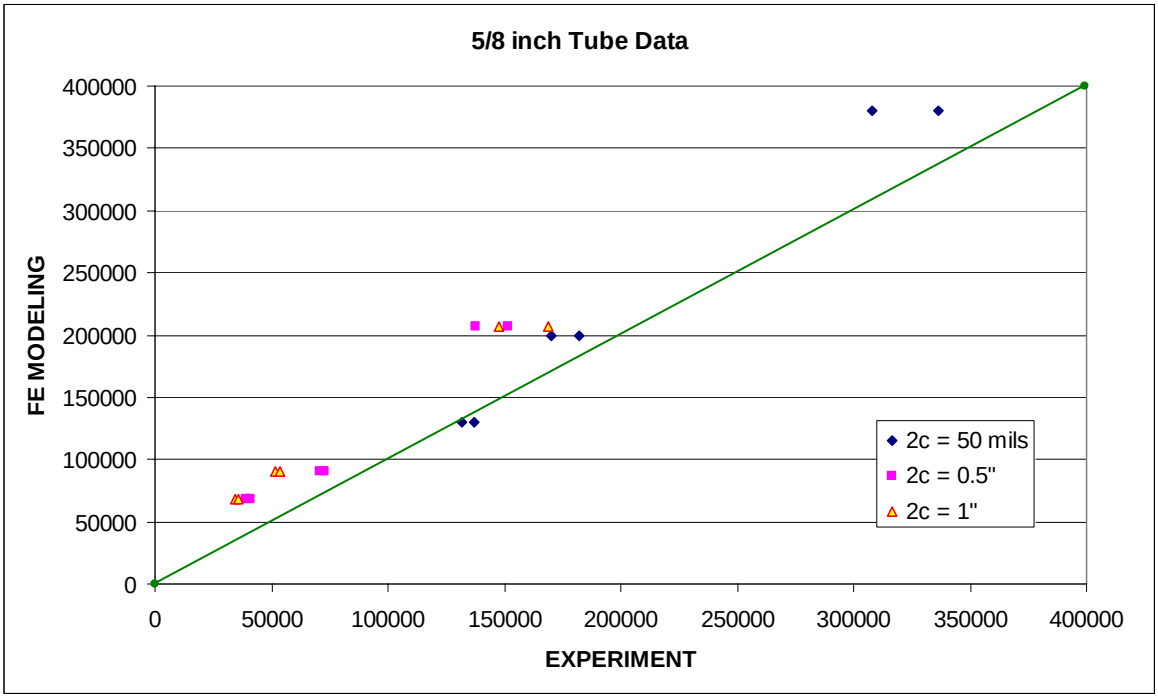

Figure C. Comparison of fatigue lives of 5/8 inch titanium tube between finite element modeling prediction and experiments.

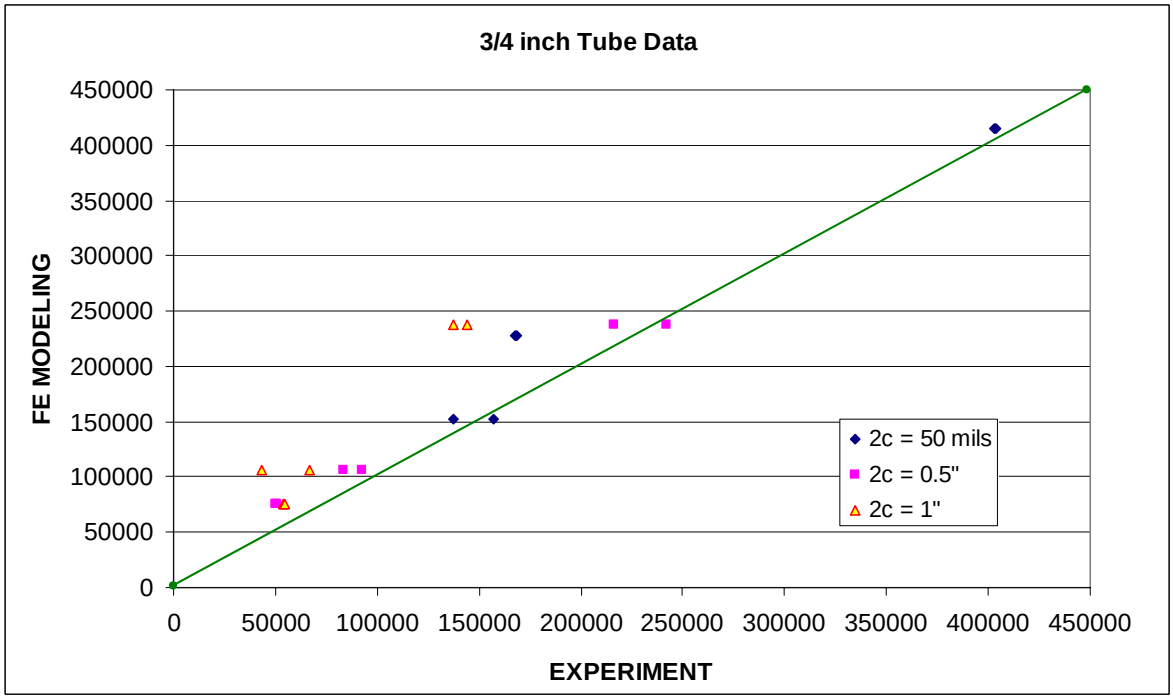

Figure D. Comparison of fatigue lives of 3/4 inch titanium tube between finite element modeling prediction and experiments.

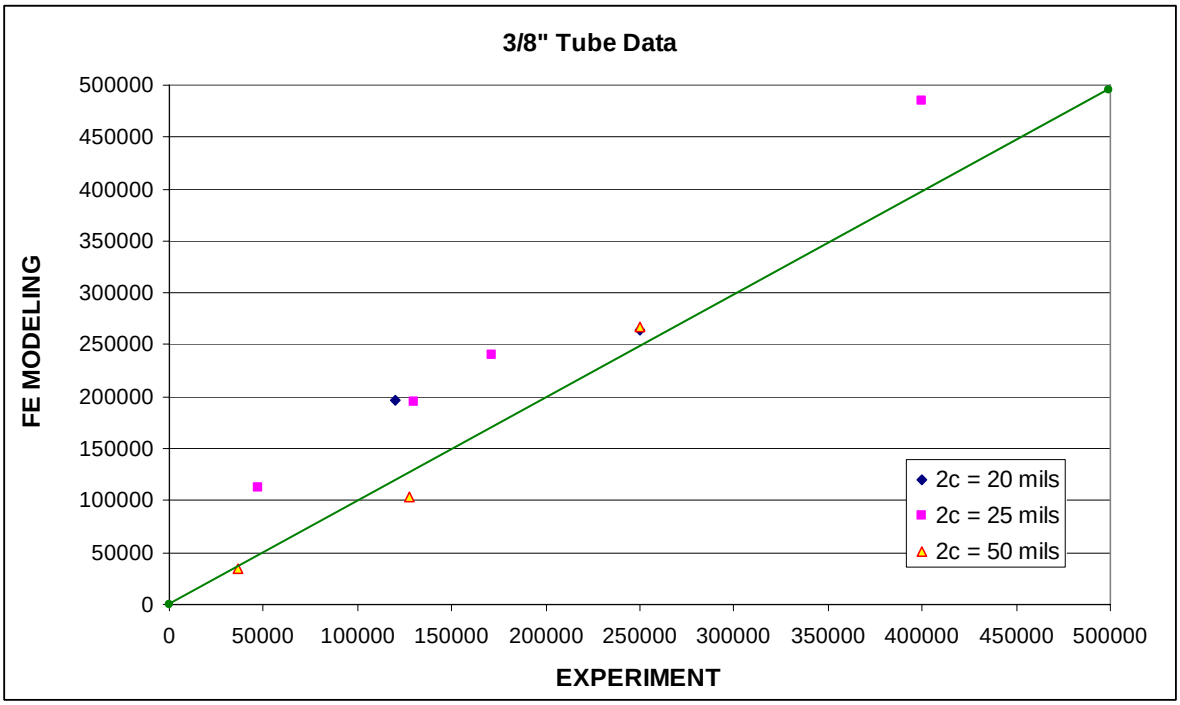

Figure E. Comparison of fatigue lives of 3/8 inch titanium tube between finite element modeling prediction and experiments.

4 Fatigue Life Trends

Based on experimental test, the damage limit curves (fatigue life trends) of the titanium tubes are determined. Figure F shows the fatigue life of the Ti tube versus the crack depth for short notch (notch length: 0.050 inch). For long notch (notch length: 1 inch), the fatigue life trends are shown in Figure G. It is seen that for all the tube with different outer diameters, the fatigue life decreases with the increase of crack depth. The tubes with crack of 0.050 inch in length and nominal depth of larger than 0.002 inch will have reduced life cycle than expected value of 200,000. And the ¼ inch OD tube is the worst case among all others.

These graphs along with damage limit inspection tool could be used by the fleet maintainer for removing unsafe tubes from the aircraft.

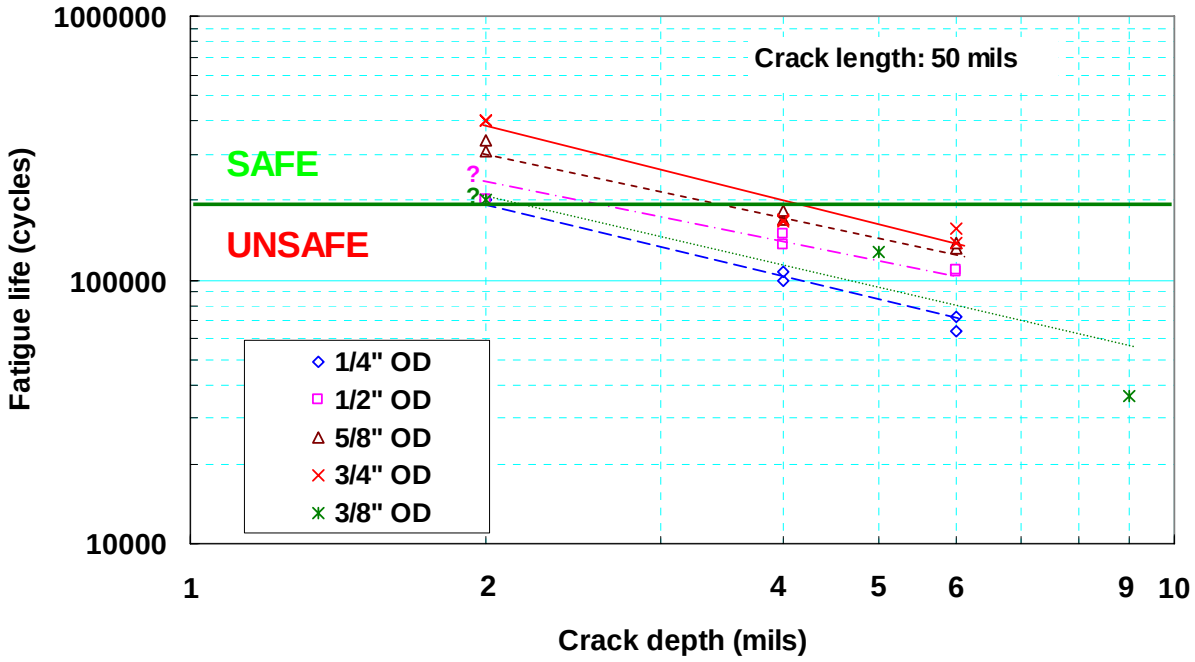

Figure F. Fatigue life trend (for tubes with a short crack of 0.050 inch).

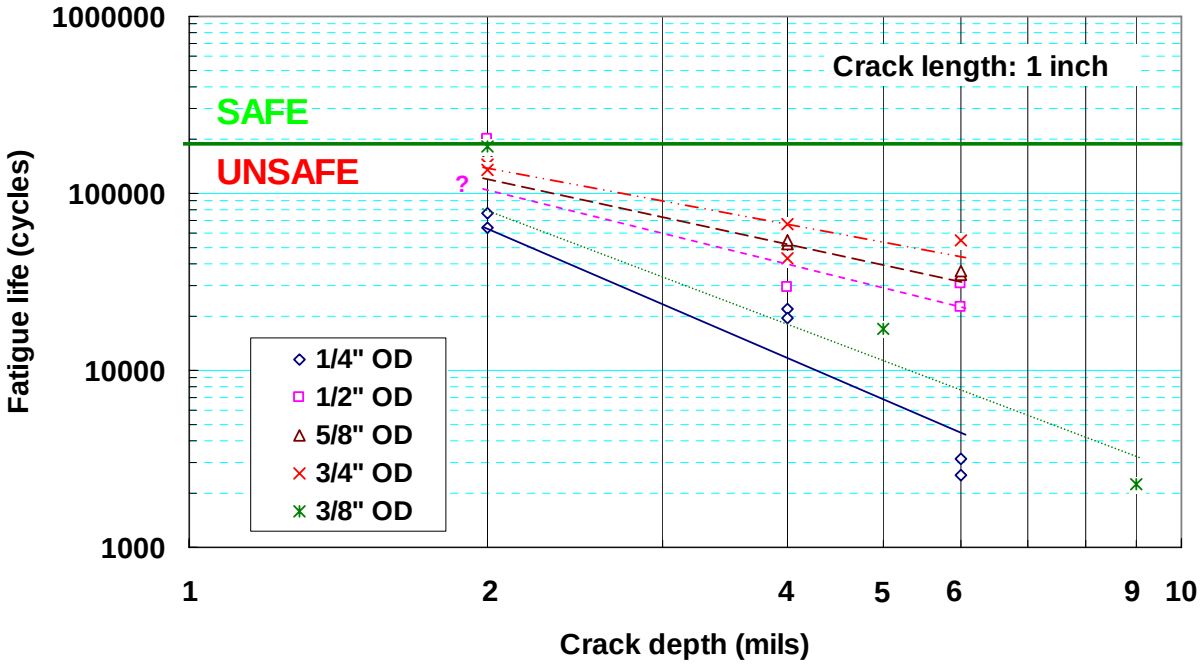

Figure G. Fatigue life trend (for tubes with a long crack of 1 inch).

5 Future Work

Following recommendations are made based on this study:

1. Determination of damage limits for bent tubes. Initial results indicate even shorter fatigue life for bent tubes as compared to straight tubes;
2. Integration of NAVAIR-UVa team results with Bell-Boeing data;
3. Demonstration of crack depth measurement system:
    a. Replica method;
    b. Micrometer gauge with sharp tip;
    c. Optical method.
4. Improved inspection of inside surface of tubes and Ti tube material.

DAAD-19-99-1-0277

FINAL PROJECT REPORT – Part I

Experimental Damage Limits Study of Laser Micromachined Notched Straight Ti-3Al-2.5V Tubes

Yaomin Lin, Teh-Hwa Wong and Mool C. Gupta
University of Virginia
Kevin Woodland, Tim Grose, Tom Spidel, Bill Stone and Michael Yu
NAVAIR V-22 Program Office
Bob Taylor and Charles Lei
NAVAIR Materials
Reanne Williams
NAVAIR Hydraulics

Submitted to
Mr. Kevin Woodland
NAVAIR V-22 Program Office
Patuxent River, MD 20670

Executive Summary

Determination of damage limits for Ti alloy hydraulic tubes is important to insure the safety of the V-22 aircraft over long period of operation. The damage limits for straight Ti-3Al-2.5V tubes with outer diameter (OD) of 3/8 inch and tube wall thickness of 0.032 inch were summarized in a previous report. In this report, we present the fatigue life cycle (internal impulse pressure) test results and give the fatigue life trends for the straight Ti alloy tubes with ODs of ¼ inch, 3/8 inch, ½ inch, 5/8 inch and ¾ inch with the corresponding tube wall thicknesses of 0.022 inch, 0.032 inch, 0.043 inch, 0.054 inch and 0.065 inch, respectively. Presented results are worst case life cycles for short and long cracks or scratches based on sharp notch studies. Detailed information of laser micromachining process for generating the sharp notches on external surface of the tubes is described. Post-fracture crack profiling results for both short and long cracks are also presented in this report. Periodic inspection of Ti alloy tubes in combination with damage limit curves will provide a powerful tool to fleet maintainer for change of unsafe tubes.

Principal Investigator: Prof. Mool C. Gupta
Department of Electrical & Computer Engineering, University of Virginia, Charlottesville, Virginia 22904, Email: mgupta@virginia.edu, Phone: 757-325-6850, Fax: 757-325-6988

May 15, 2007

1 Introduction

Defects (flaws), such as gouges, scratches, fretting, dents, and pits on external surface of in-service titanium alloy tubes in a V-22 tilt rotor aircraft can reduce total life cycles for operation. Assessment of allowable in-service tube damage is therefore important to avoid fatigue failure and sustain the aircraft for long-term operation. The focus of the "Damage Limits Study for Straight Ti-3Al-2.5V Tubes" project is to assure the safety of the aircraft and provide airframe maintainer and quality personnel tools to determine if the tube should be removed from the aircraft if a damage is noted. By laboratory testing, damage limit curves or trends of the fatigue lives of the titanium tubes can be developed and applied to determine the acceptable defect depth and length to avoid hydraulic leak failure within required service hours.

In the first phase of the project, five cases have been put forward and applied to determine the damage limit curves of the straight tube with 3/8" outer diameter (OD) and 0.032" tube wall thickness (TWT). The cases are: 1) determine the worst type of flaw that makes a tube experience the shortest fatigue life to failure. The determination should be under the realistic condition of the in service flaw depth and length; 2) conduct internal impulse pressure tests for the tubes with the worst type of flaw with different flaw profiles (i.e., combination of flaw depth and length) to experimentally determine the relationship between the flaw profile and fatigue life to failure. Impulse test was chosen to simulate the actual pressure cycles used in the flight operation of the aircraft.; 3) determine stress and strain distributions near the worst type of flaw when the tube is subjected to inner impulse pressures that are used in the tests; 4) perform fatigue life prediction of the tube based on the predicted stresses and strains and validate the predicted life with experimental impulse test data; and 5) determine flaw profile combinations of the tube that can resist 200,000 cycle internal impulse pressure and generate the damage limit curve for

the tube. Life cycle of 200,000 dynamic pressure levels is assumed to correspond to about 10,000 hours of flight time.

Based on stress analysis, sharp and deep scratches on outer tube surface and along the tube axis (see Figure 1) can be considered as the most severe defect as compared to the other detected outer surface damages with the same defect depth [1]. A longitudinal (axial) sharp notch on external surface of a tube was, therefore, used as the defect to determine the damage limit of the tube. Figure 2 gives the damage limit curves for 3/8" OD × 0.032" TWT tube based on fatigue crack growth life modeling and total fatigue life modeling. The comparison of damage limit curves for 3/8" OD × 0.032" TWT tube with experimental life data from impulse pressure tests for tubes with a short notch and a long notch are shown in Figures 3(a) and 3(b) respectively [1]. Modeling and experimental results indicate that laser micromachining (LMM) is an appropriate tool for introducing a pre-crack to study crack growth characteristics of Ti-3Al-2.5V [2].

In this report, the impulse pressure test results for straight tubes with ¼" OD × 0.022" TWT, 3/8" OD × 0.032" TWT, ½" OD × 0.043" TWT, 5/8" OD × 0.054" TWT, and ¾" OD × 0.065" TWT are presented and analyzed. The failure analysis based on optical microscopy and scanning electron microscopy (SEM) is also presented. The results of crack profiling analysis provide valuable information about crack growth path for fracture mechanics study of titanium tubes with both short and long notches.

2 Internal impulse pressure tests

Impulse pressure tests were performed by NAVAIR Hydraulics Lab and NAVAIR Materials Lab to experimentally obtain the fatigue life of Ti-3Al-2.5V tubes with an axial LMM

notch on their external surface and to get the trend of the fatigue life of the titanium tubes based on the limited test data. The impulse internal pressure test procedure is described in ARP 603 manual [4]. The tubes were purchased from Haynes International Inc. and in cold worked and stress relieved condition (heat treated @995^{o}F/2 hr). The chemical composition of the tube material is shown in Table 1 [3].

2.1 Test sample preparation

Tube samples for the internal impulse pressure test were prepared using the method of laser micromachining to generate the specific notch dimensions on their external surfaces. Figure 4 illustrates the LMM experimental setup. In order to study the fatigue life of the tubes with pre-notched flaws, it is important to get the test samples with the specific notch dimensions (length and depth) since the fatigue life of the tubes is determined by the characteristics of the flaws under the same test conditions. As a result, large number of experiment were performed to obtain the laser processing parameters for achieving the desired notch lengths and depths before the laser notches were put on the "real" samples tested by NAVAIR hydraulic internal impulse pressure tests.

The laser notch length and depth were characterized and the relationship between the notch dimension and the laser processing parameters (laser power, repetition rate, scanning time, etc.) were studied in the experiment. Two stainless steel sheet plates were arranged in a certain distance (the distance was to be adjusted according to the desired notch length) away from each other and put in front of the test sample to block the laser beam in order to control the length of the notch that was generated by laser on the outer surface of the titanium tubes, as shown in Figure 4 (c). For characterization of the notch depth, the test tubes were cross-sectioned, polished

and investigated under an optical microscope. Figure 5 shows the facilities used for the cross-sectioning and polishing processes. The notch depth was measured under the optical microscope. If the measured and the desired notch depths were not in a good agreement, then another test was carried out with the adjusted laser parameters, and a desired notch was generated. This process was repeated until the notch depth was very close to the specific value. And then the laser parameters were used to generate the notches on the "real" tube samples that were to be tested in the Hydraulics and Materials Labs at NAVAIR.

The processes of the test and experiment can be summarized as follows:

1) Adjust the distance between the two sheet plates (laser beam blocker), load the tube sample on the fixtures and put a laser notch on its outer surface;
2) Measure the notch length on the tube sample (for short notch, the measurement was taken under an optical microscope);
3) Readjust the laser beam blocker, choose another position on the sample and put another laser notch;
4) Repeat the above processes 2 ~ 3, until the desired notch length is obtained;
5) Get the cross section of the tube sample at the notch, polish the cross-sectioned surface and measure the notch depth under the optical microscope;
6) Choose another position on the tube sample, adjust the laser parameters and put another laser notch (the length of the notch is kept the same);
7) Repeat the above processes 5 ~ 6, until the desired notch depth is obtained;
8) Load the test tube sample and put the laser notch at around the center using the parameters determined by the above processes.

Totally eighty-four 8 inch long tube samples were laser micromachined to generate the specific laser notches on the external surfaces. Figure 6 shows some of the test samples prepared using LMM. A top and cross-sectional view of the laser notch is shown in Figure 7.

To experimentally study fatigue life of the tubes with a short axial LMM notch, two notch lengths were chosen: 0.020" and 0.050". For study of the tubes with a long axial LMM notch, another two notch lengths were selected: 0.5" and 1". Three notch depths were developed for the tube fatigue life study: 0.002", 0.004" and 0.006". The measured notch width was approximately 0.006" for both the short and long notches (Figure 7). Two samples were prepared for each specific notch dimension.

Twenty-four tube samples with ¼" OD × 0.022" TWT were prepared with notch depths of 0.002", 0.004" and 0.006" respectively, combined with notch lengths of 0.020", 0.050", 0.5" and 1" respectively.

For ½" OD × 0.043" TWT tube, there were 24 samples prepared with notch depths of 0.002", 0.004" and 0.006" respectively, combined with notch lengths of 0.020", 0.050", 0.5" and 1" respectively.

Since larger sized tubes (with a larger ODs) have a larger tube wall thickness (TWT), it was expected that the larger the OD of the tube, the longer the fatigue life of the tube if the dimension of the notch on the external surface were the same. This has been verified by the experimental investigation. It was regarded that it's unnecessary to perform the life cycle test for the larger sized tube samples with a short notch of 0.020"-long because they would resist the life cycle of 200,000 dynamic pressure levels. In order to save test resources and time, for the larger sized tubes such as 5/8" OD × 0.054" TWT and ¾" OD × 0.065" TWT, only 18 samples were

prepared for each size. The notch depths were 0.002", 0.004" and 0.006" respectively, with combined notch lengths of 0.050", 0.5" and 1" respectively.

Table 2 lists the dimensions of laser micromachined notches on tubes of ¼" OD × 0.022" TWT, ½" OD × 0.043" TWT, 5/8" OD × 0.054" TWT and ¾" OD × 0.065" TWT respectively. The Young's modulus, Poisson's ratio, and yield strength of the Ti alloy tube material are listed in Table 3.

2.2 Impulse pressure tests

To experimentally evaluate fatigue life to failure of the LMM-notched tubes, impulse pressure tests were carried out based on SAE Aerospace Recommended Practice 603 [4]. The pressure profile is shown in Figure 8. The surface quality was checked and no surface crack was observed. The nominal pressure of 5000 psi and the maximum impulse pressure of 7500 psi were used for all notched tubes. Table 4 shows the controlled maximum and minimum pressure values. A tube was considered to fail when a crack grew up to its interior surface and fluid inside the tube was observed to leak from the crack.

3 Post-fracture analysis

The tube post-fracture analysis based on scanning electron microscopy (SEM) images can provide detailed information concerning the crack pattern, crack growth path etc. The information is very useful to fracture mechanics study.

3.1 Post-fracture analysis based on scanning electron microscopy

Each failed tube was cut near two ends of the final crack and opened along the crack surface. Each surface was examined using either optical microscopy or SEM. Figure 9 shows some short LMM notches (notch length is less than or equal to 0.050") on the tube. Flat crack surface was observed from every failed tube. It is seen that all cracks initiate at the notch roots and grow in both radial and axial directions. It is interesting to see that the crack growth rates in the radial and the axial directions are almost the same for the short LMM notch, whereas for the long LMM notch, the crack growth behaves totally different.

Figures 10 and 11 show the crack surfaces of the tubes with a long LMM notch (notch length is 0.5" or 1"). The following observations were made from the SEM images of the failed tubes with the long LMM notches: 1) fatigue crack initiates along the whole notch root; 2) crack grows much faster around the center of the notch than around the edges; 3) there is a apparent swelling of the tubes with a one-inch-long notch (Figure 12), which means that the tubes with longer notch (one-inch-long) experienced rapid failure during the hydraulic cycling test; (4) no crack growth was observed along the length of the tube.

3.2 Summary of post-fracture analysis

Based on the optical microscopy and SEM images, the tube failure analysis was performed and the following observations can be made:

1. Failure of the tube with a short LMM notch (less than or equal to 0.050") or a long LMM notch (length equals to 0.50" or 1") behaves totally differently;
2. For tubes with a short LMM notch, the fatigue cracks initiate at the notch roots and grow in both radial and axial directions in almost the same rate;

3. For tubes with a long LMM notch, the fatigue crack still initiates along the whole notch root but it grows much faster around the center of the notch than around the edges of the notch. Moreover, for some tubes with a one inch long notch, apparent swelling is observed which indicates the tubes experienced the rapid failure during the impulse pressure cycling test.

4 Determination of damage limits of titanium tubes

4.1 Impulse pressure test results and analysis

The impulse pressure test results for the 1/4" OD × 0.022" TWT, 3/8" OD × 0.032" TWT, 1/2" OD × 0.043" TWT, 5/8" OD × 0.054" TWT and 3/4" OD × 0.065" TWT tubes are listed in Tables 5, 6, 7, 8 and 9 respectively. The comparison of the desired and the measured notch depth and length is given in Table 10. There are a few differences between the measured and the desired notch dimensions, these come from the measurement errors using the current method of notch depth characterization as described in Section 2.1. The method compared the measurements of the notch depth and the tube wall thickness in the optical images to get an estimation of the notch depth based on the TWT was supposed to be a constant but actually it is not. The tolerance data for Ti-tubing are listed in Table 11.

From Tables 5 ~ 9, it is seen that, 1) with only a few exceptions, the fatigue life to failure increases with increase in tube OD and TWT; 2) for a given notch depth, the longer the notch length, the shorter the tube's fatigue lives; 3) for a given notch length, the deeper the notch depth, the shorter the tube's fatigue lives. The second observation is more clear as seen from Figures 13, 14, 15 and 16, which illustrate the relationship between the notch length and the life to failure for

the 1/4" OD × 0.022" TWT, 1/2" OD × 0.043" TWT, 5/8" OD × 0.054" TWT and 3/4" OD × 0.065" TWT tubes, respectively.

The relationship between the notch depth and the life to failure for the 1/4" OD × 0.022" TWT, 3/8" OD × 0.032" TWT, 1/2" OD × 0.043" TWT, 5/8" OD × 0.054" TWT and 3/4" OD × 0.065" TWT tubes is shown in Figures 17, 18, 19, 20 and 21, respectively. The third observation made in the last paragraph is clearly seen in these figures, i.e., for a given notch length, the deeper the notch, the shorter the fatigue life.

From Figures 13 ~ 21, it is seen that the life cycle is dependent upon the notch length and notch depth. The relationship among the life cycle N of the tube with an axial notch of length L (in mils) and depth D (in mils) can be expressed in the following equation

$$N \propto L^m D^n \tag{1}$$

Where m and n are exponents. For a specific tube, with a given notch length or notch depth, the n or m is negative and equals to the slope in the log-log graphs.

Figures 22 and 23 show the fatigue life versus tube OD and tube TWT, respectively. It is obvious that along with the increase of the tube size (OD and TWT), the fatigue life to failure of the tube increases. The slope in the log-log graph seems a constant, regardless of the dimensions of the notch on the tube. The relationship between the life cycle N of the tube and the tube OD d (in mils) thus can be expressed as

$$N = a * d^z \tag{2}$$

Where a is a constant and z is the exponent.

4.2 Summary of experimental damage limits study

Our previous research has shown that scratches along the tube axis are the most severe defect compared to the other detected damages in the fleet aircraft. The LMM notch is sharper at its notch root as compared to any detected fleet surface flaw. The LMM notch along tube axial direction is the worst in terms of fatigue life of the tube. Impulse pressure tests have been performed on straight tubes of various sizes with the LMM generated longitudinal notch of various dimensions. From the test result analysis, the following observations can be made:

1. Tubes of any size with any type of flaw detected in fleet aircraft can withstand over 200,000 impulse pressure cycles (nominal pressure: 5,000 psi, maximum internal impulse pressure: 7,500 psi) if the flaw length is less than or equal to 0.020";
2. Tubes of any size can withstand over 200,000 impulse pressure cycles if the flaw depth is no more than 0.002" and flaw length is less than or equal to 0.050";
3. For any specific notch depth, the longer the notch along the axial direction of the tube, the shorter the tube's fatigue life;
4. For any specific notch length, the deeper the notch, the shorter the fatigue life of the tube.
5. Fatigue life cycle to failure of the tube increases along with the increase of tube size (OD). This is attributed to the increased tube wall thickness (TWT).
6. Fatigue life cycle of pre-notched tube changes exponentially with the variations of the notch length, notch depth and the outer diameter of the tube.
7. Long cracks (> 0.050" in length):
    1) For 1/4 inch tube size, life cycles is only ~80k cycles for 2 mil notch depth and will have even shorter life cycles for bent tubes;

2) For 1/4 inch tube size, life cycle reduces to ~25k cycles for 4 mil notch depth and will have even shorter life for bent tubes.

As a result, significant attention needs to be paid to 1/4 inch tubes.

REFERENCES

1 Li, B., Wong, T.H., Gupta, M. C., Spidel, T., Grose, T., Stone, B., Yu, M., Taylor, B., Lei, C., and Williams, R., "Damage Limits Study for Straight Ti-3Al-2.5V Tubes with 3/8" OD and 0.032" Wall Thickness," *NAVAIR Project Report*, 70 pp., 2005.

2 Li, B. and Gupta, M. C., "Crack Growth Life of Ti-3Al-2.5V Tubes Under Internal Impulse Pressure," *Materials Science and Engineering A*, Vol. 431, pp. 146-151, 2006.

3 HAYNES International, Inc. Report of physical, chemical & mechanical properties, Test # 10125.

4 Society of Automotive Engineers, "Aerospace Recommended Practice 603 – Rev. F," Warrendale, PA 15096, 1985.

5 Pregger, B., "Titanium Tube Investigation – In-Service Tube Damage," Presentation by NAVAIR Material, March 23, 2004, Applied Research Center, Old Dominion University.

6 Li, B., Gupta, M. C., Stone, B., Spidel, Yu, M., Williams, R., Taylor, B., and Lei, C., "Stress Analysis and Fatigue Life Prediction of Laser and Electrical Discharge Machine-Notched Ti-3Al-2.5V Tubes," under submission, 2006.

Figure 1 The most severe defect on external surface of in-service titanium alloy tubes – the scratch [5].

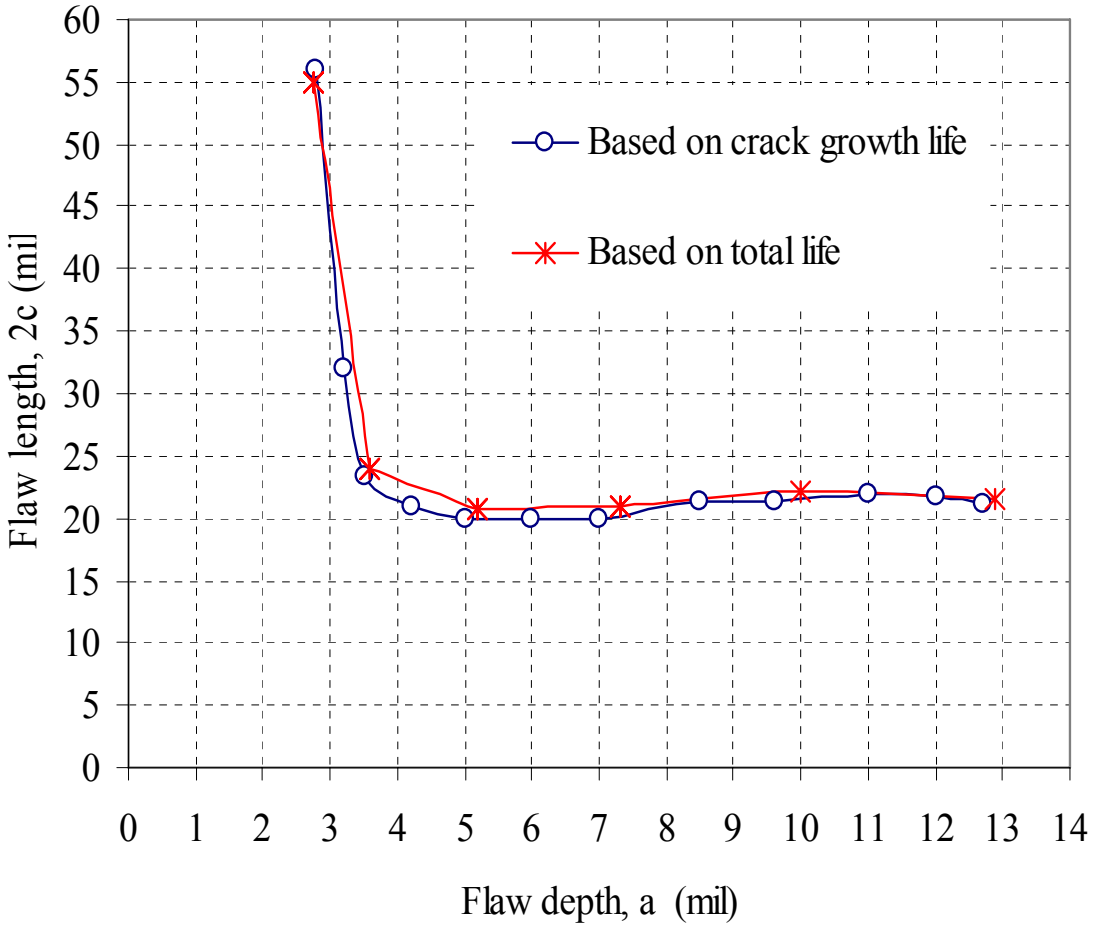

Figure 2 Damage limit curves based on fatigue crack growth life modeling and total fatigue life modeling for 3/8" OD × 0.032" TWT tube [1].

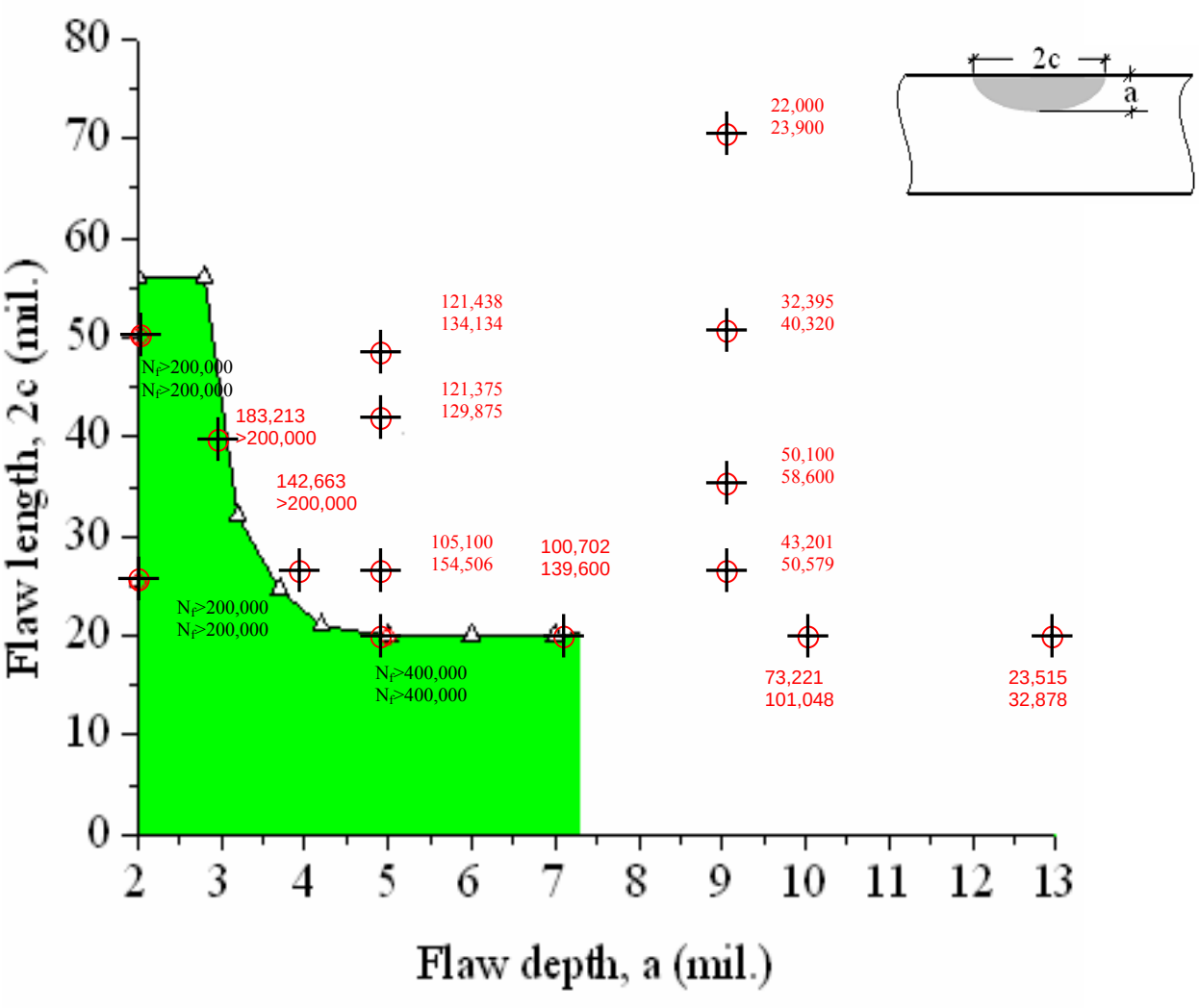

Figure 3(a) Comparison of damage limit curve for 3/8”OD × 0.032”TWT tube with experimental life data from impulse pressure tests for tubes with a short notch [1].

△ - indicates modeling data,

┼ - indicates experimental data.

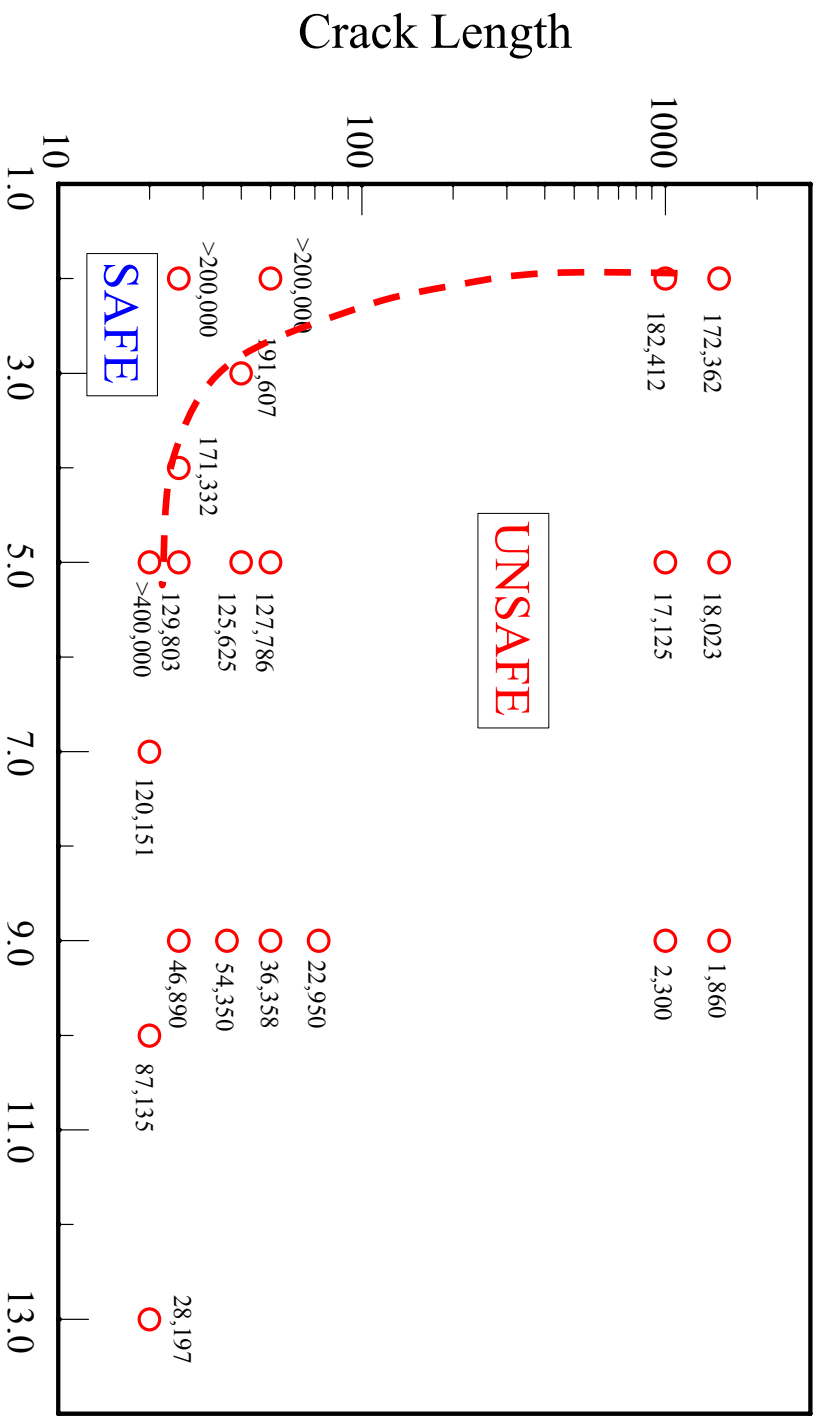

Figure 3(b) Comparison of damage limit curve for 3/8”ODx0.032”TWT tube with experimental life data from impulse pressure tests for tubes with a long notch [13].

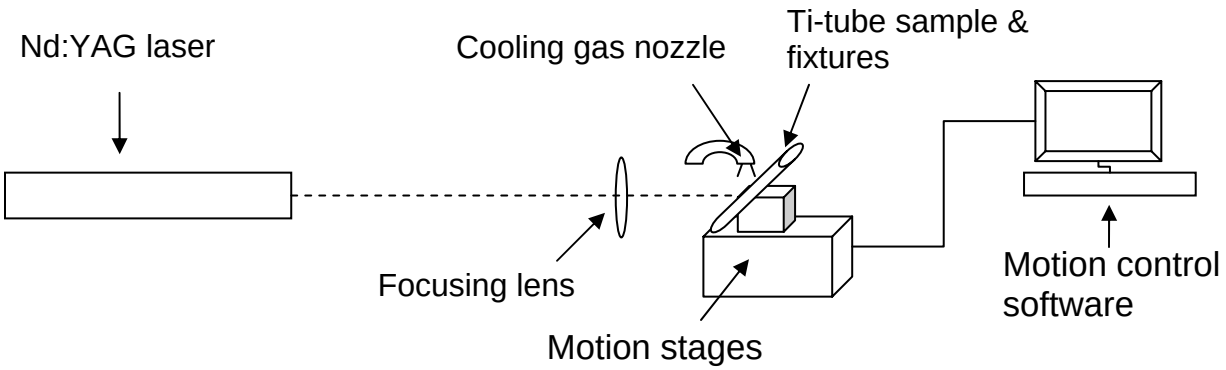

(a)

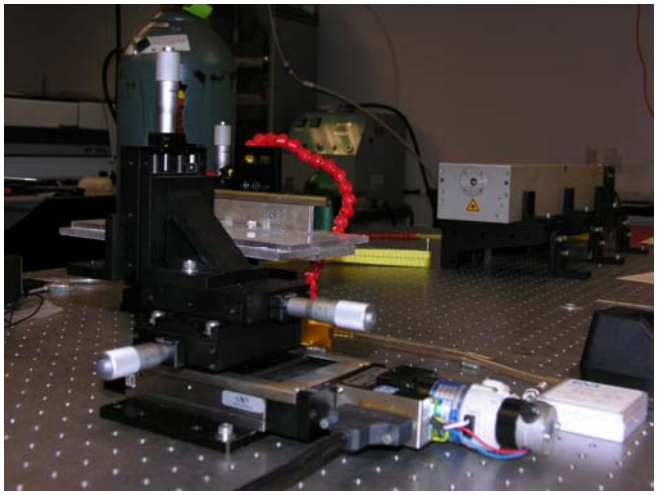

(b)

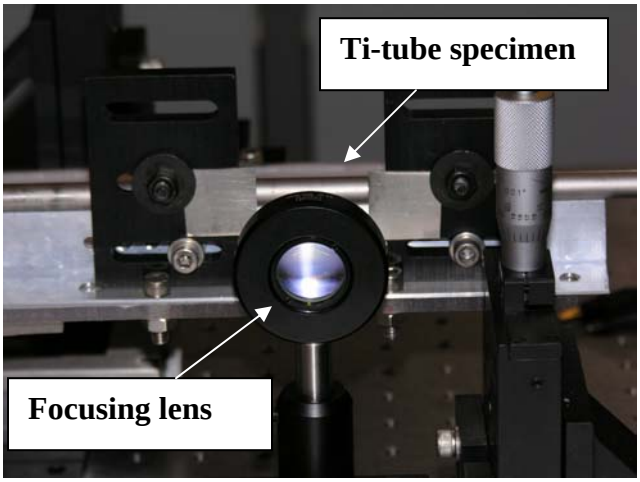

(c)

Figure 4 (a) Schematic of experimental setup; (b) photograph of experimental setup; (c) close-up of specimen fixtures and focusing lens.

(a)

(b)

(c)

Figure 5 Laboratory equipments used in the characterization of the laser notch depth. (a) automatic low speed saw; (b) manual diamond blade saw; (c) grinder / polisher.

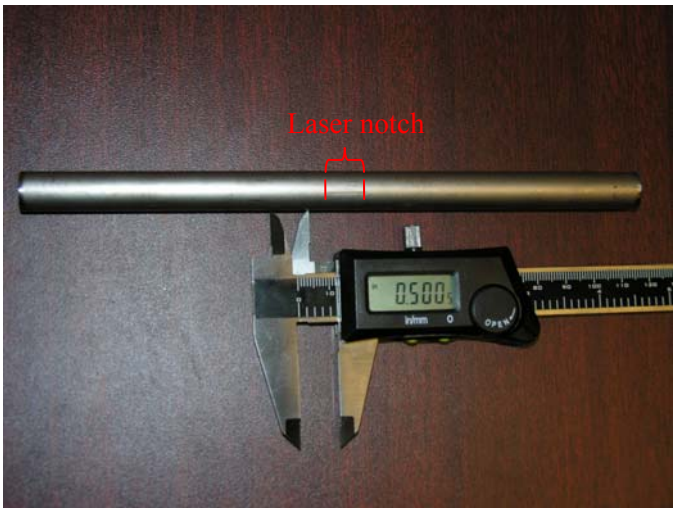

(a)

(b)

Figure 6 (a) A tube sample with a LMM notch on the outer surface (notch length: 0.5”); (b) laser micromachined tube samples.

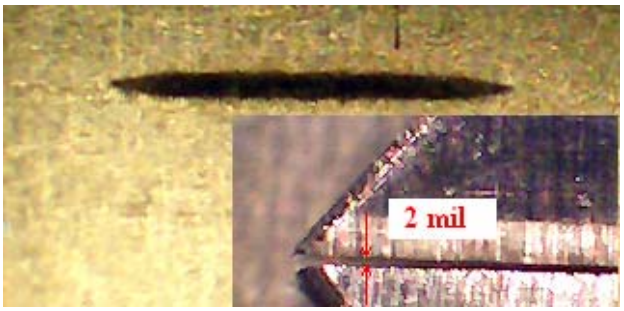

(a)

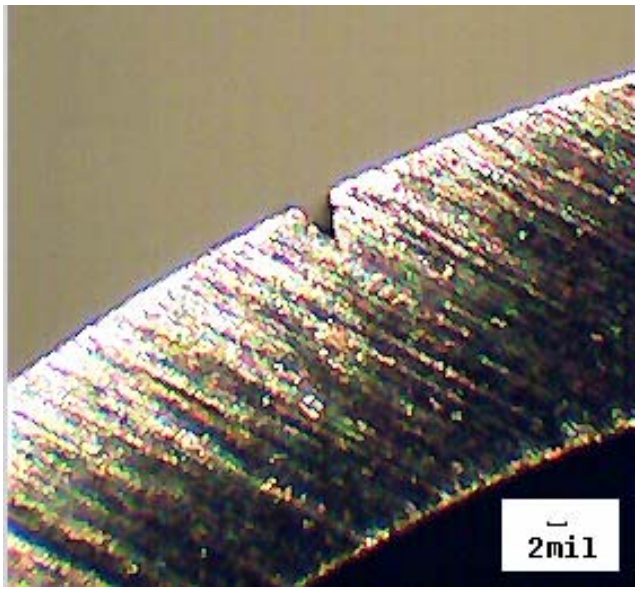

(b)

Figure 7 Laser micromachined notch. (a) view along tube axis (top view); (b) tube cross-sectional view. Approximate notch width: 0.006”.

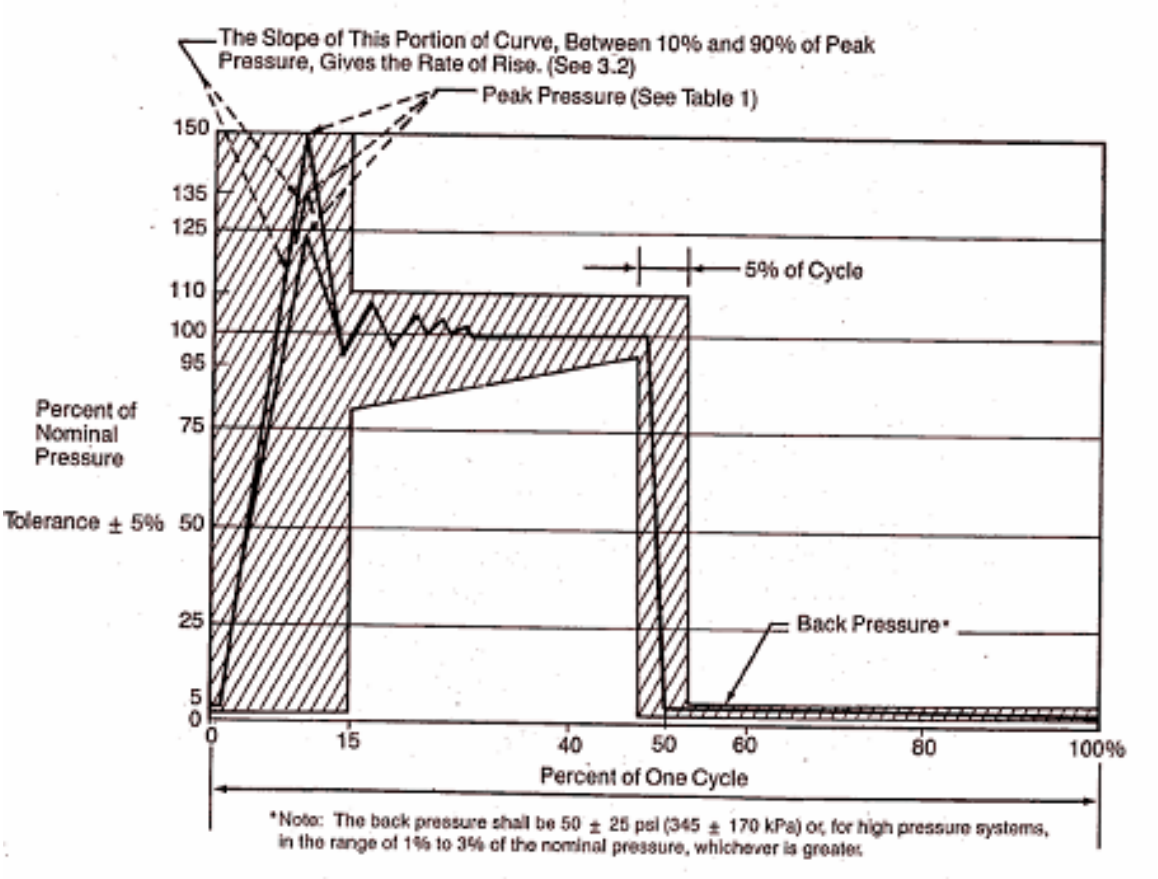

Figure 8 Schematic of impulse trace used for internal impulse pressure test program (one cycle).

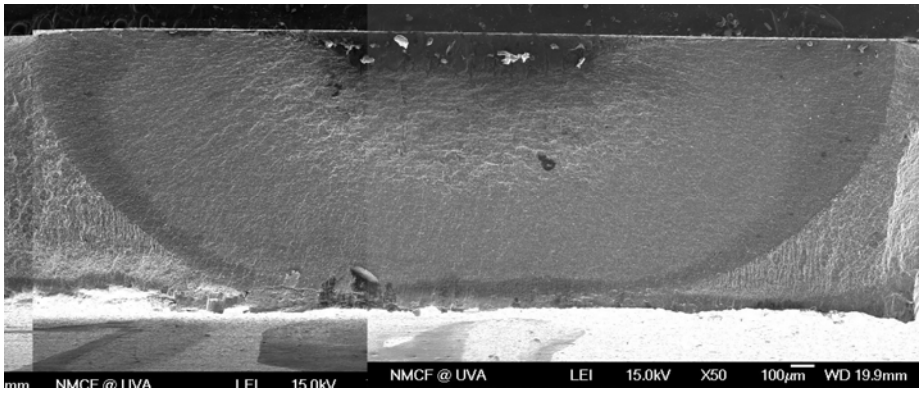

(a)

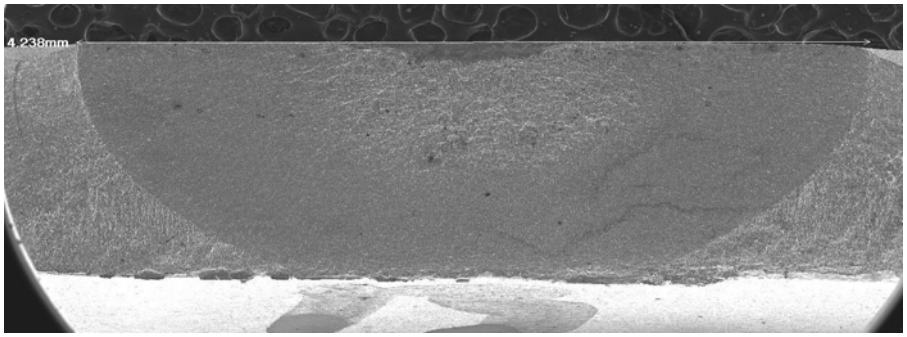

(b)

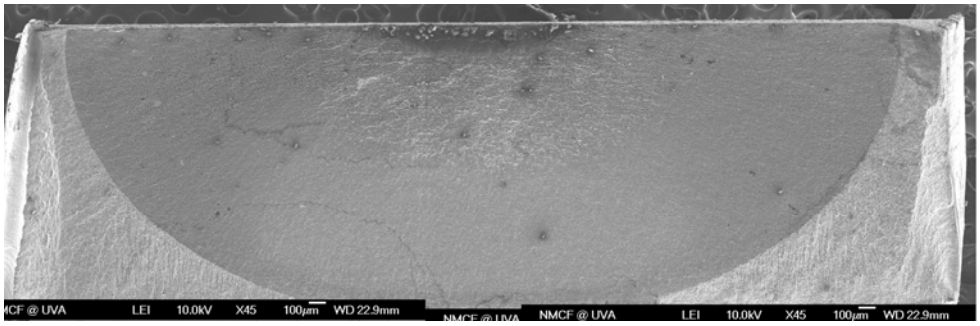

(c)

Figure 9 SEM images showing crack growth plane from the failed tubes under 5,000 psi nominal pressure. (a) ½" OD tube, notch dimension 0.006"×0.050"; (b) 5/8" OD tube, notch dimension 0.004"×0.050"; (c) ¾" OD tube, notch dimension 0.006"×0.050".

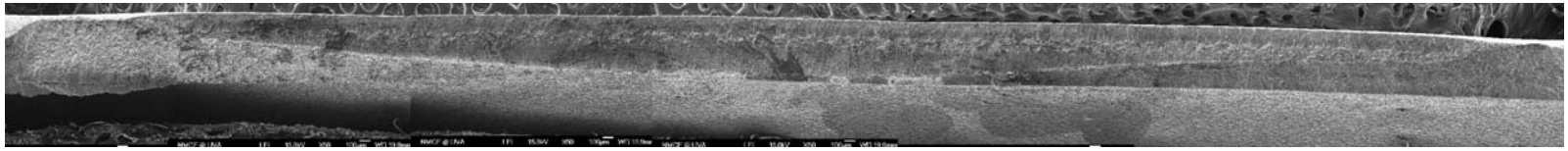

(a)

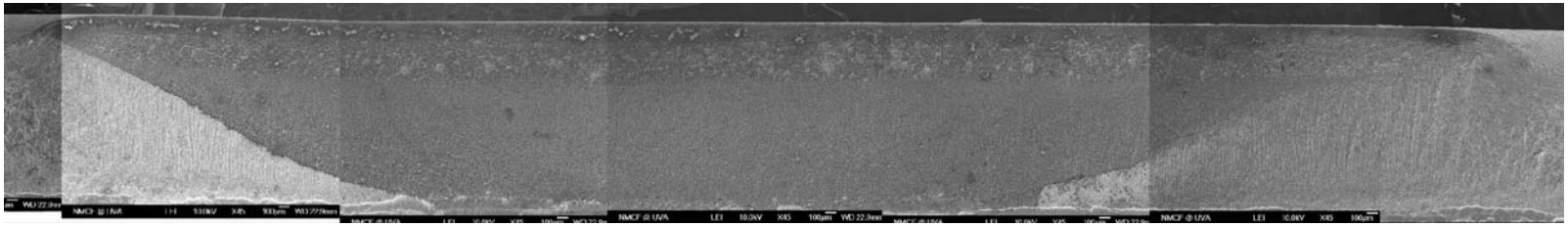

(b)

DAAD-19-99-1-0277

Figure 10 SEM images showing crack growth plane from the failed tubes under 5,000 psi nominal pressure with 0.5 inch long LMM notch. (a) 1/4" OD tube, notch depth: 0.006"; (b) 3/4" OD tube, notch depth: 0.004".

(a)

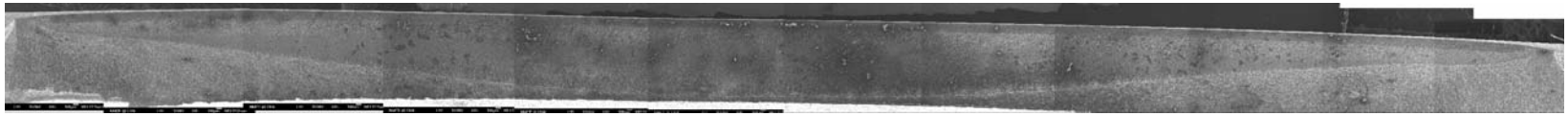

(b)

Figure 11 SEM images showing crack growth plane from the failed tubes with 1” long LMM notch. (a) 1/4” OD tube, notch depth: 0.002”; (b) 5/8” OD tube, notch depth: 0.006”.

DAAD-19-99-1-0277

(a)

(b)

(c)

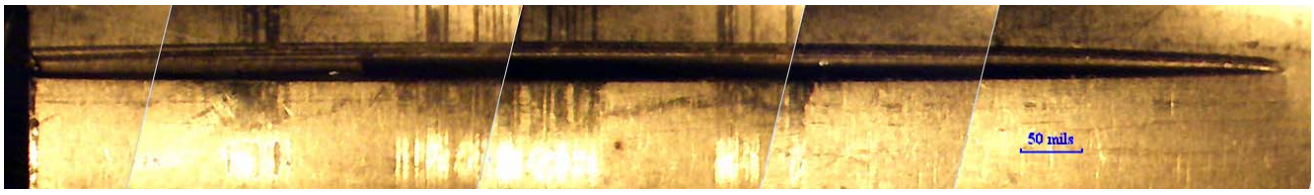

(d)

Figure 12 Tubes with 1" long notch show apparent swelling during the impulse pressure test. (a) two tested samples (both are 5/8" OD tubes with 0.006"×1" notch); (b) outer fracture surface of the ¾" OD tube (notch dimension 0.004"×1"); (c) inner fracture surface of the ¾" OD tube (notch dimension 0.004"×1"); (d) optical image of a fractured ½" OD tube, notch dimension 0.004"×1".

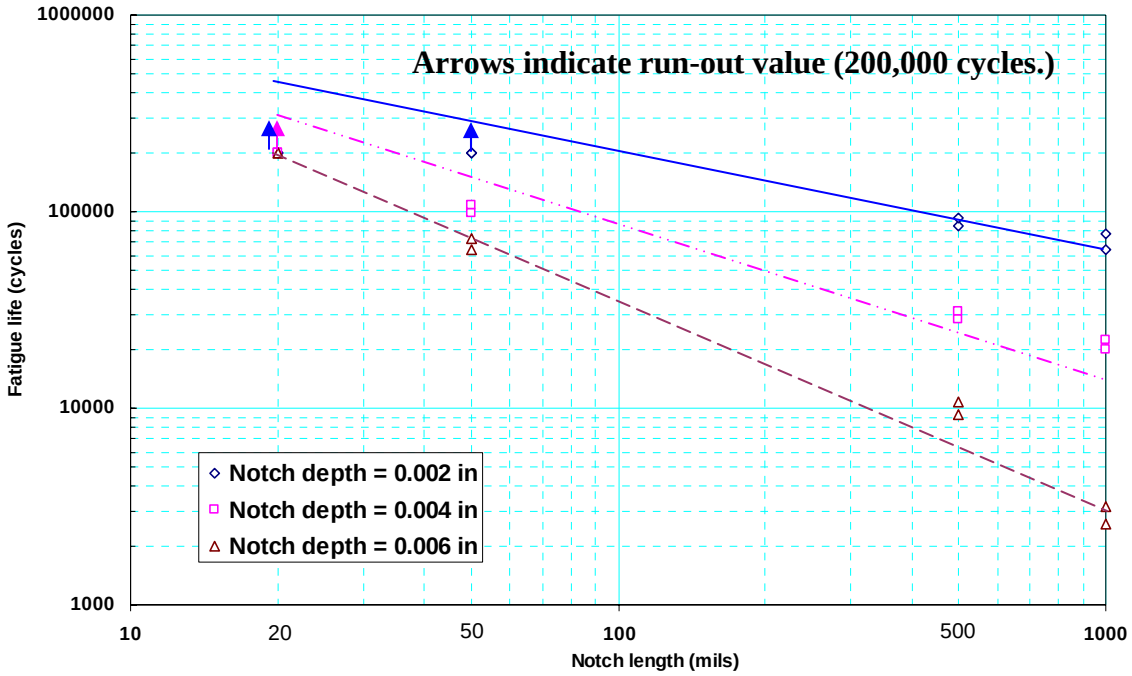

Figure 13 LMM notch length versus fatigue life cycles to failure (1/4” OD × 0.022” TWT tubes).

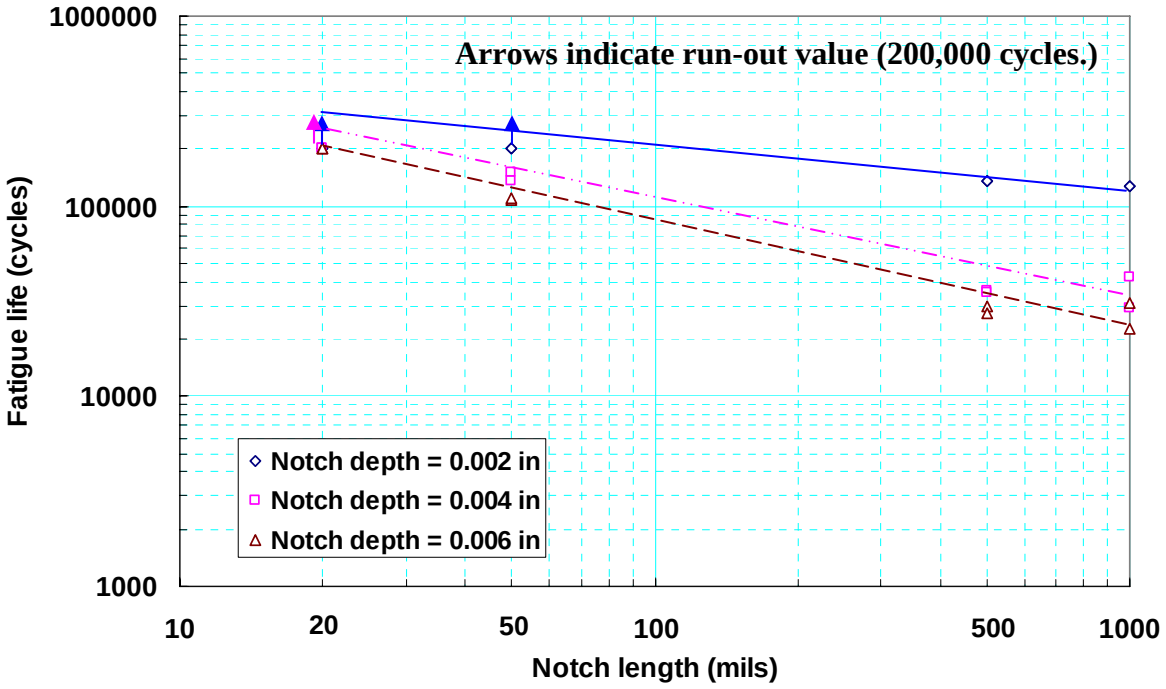

Figure 14 LMM notch length versus fatigue life cycles to failure (1/2" OD × 0.043" TWT tubes).

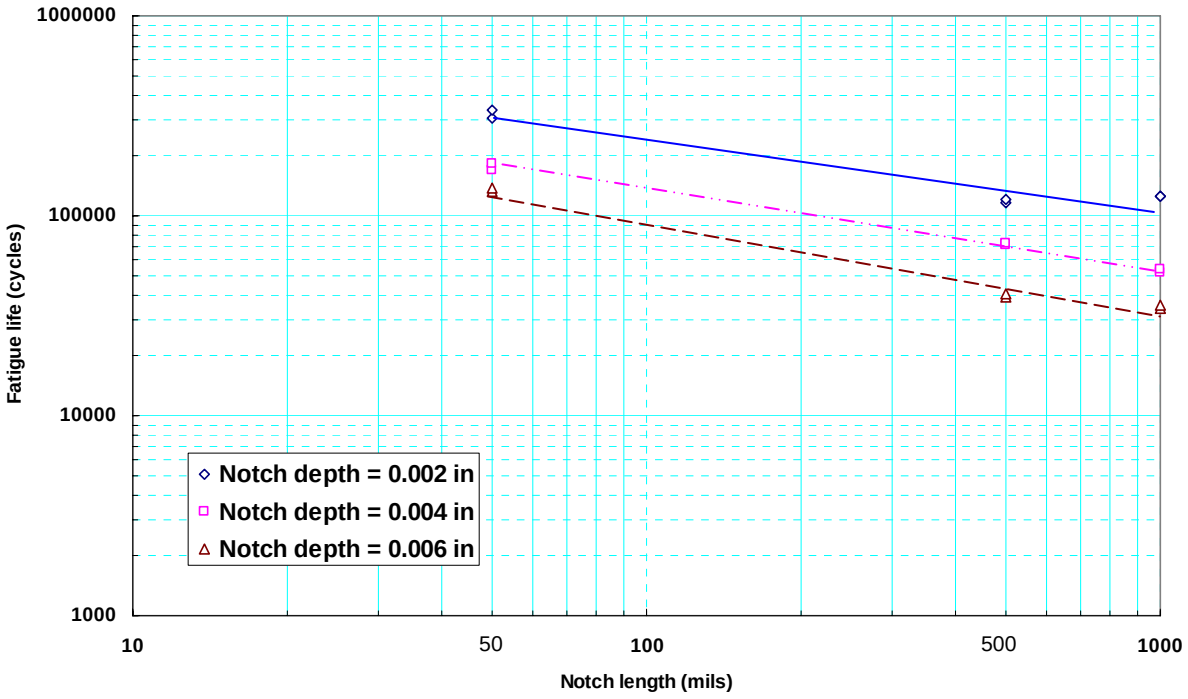

Figure 15 LMM notch length versus fatigue life cycles to failure (5/8” OD × 0.054” TWT tubes).

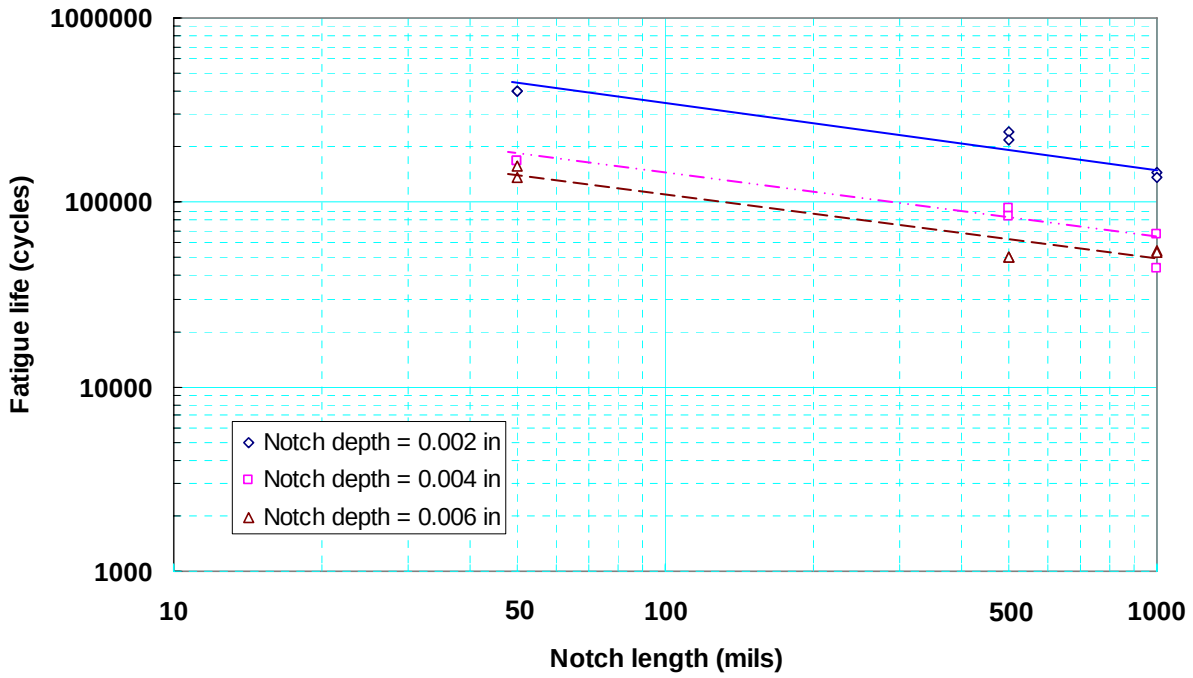

Figure 16 LMM notch length versus fatigue life cycles to failure (3/4" OD × 0.065" TWT tubes).

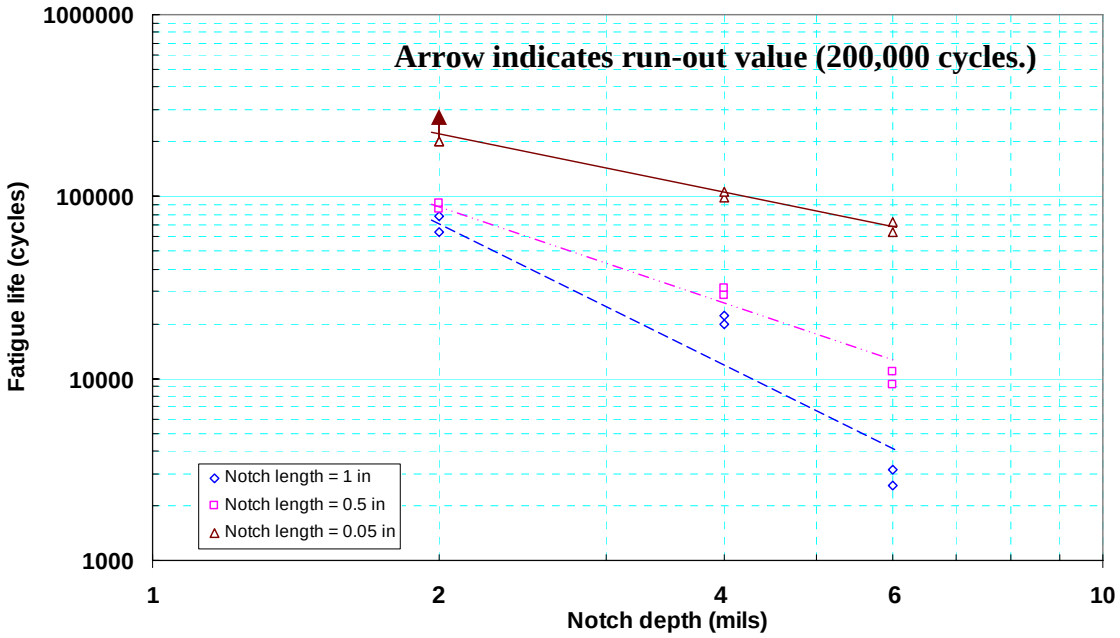

Figure 17 LMM notch depth versus fatigue life cycles to failure (1/4” OD × 0.022” TWT tubes).

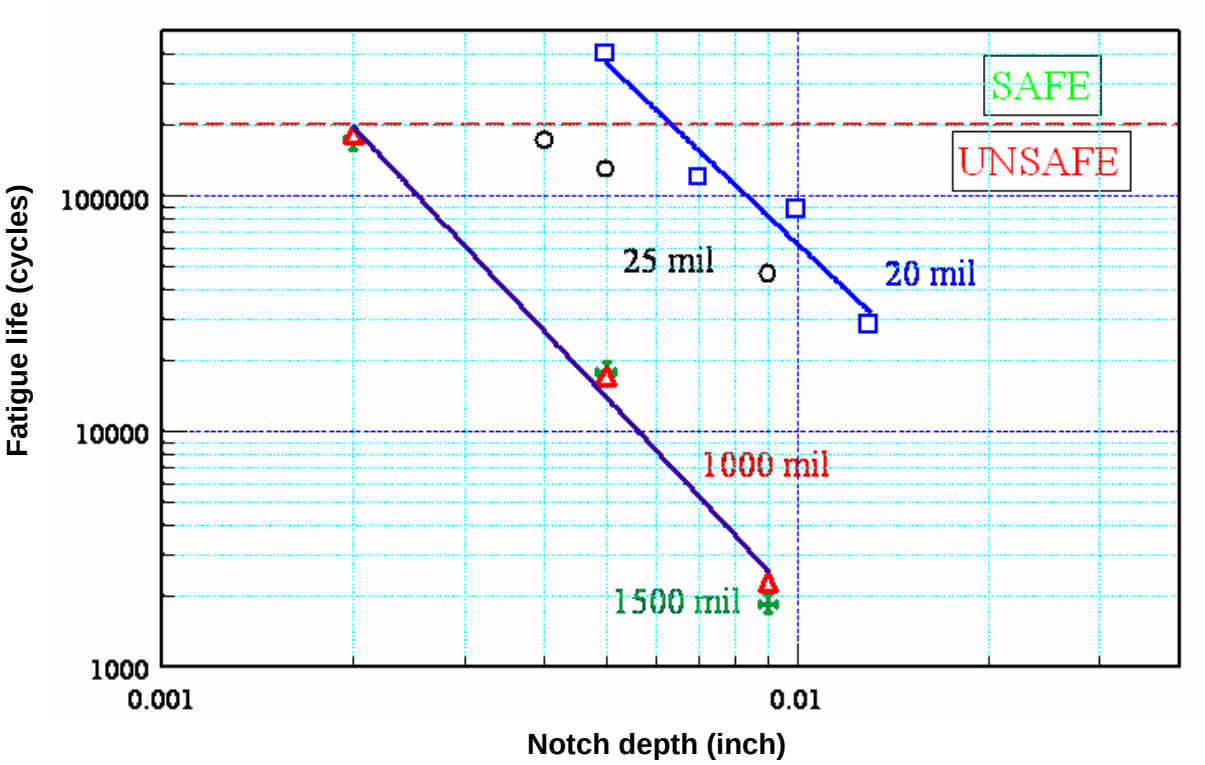

Figure 18 LMM notch depth versus fatigue life cycles to failure (3/8” OD × 0.032” TWT tubes).

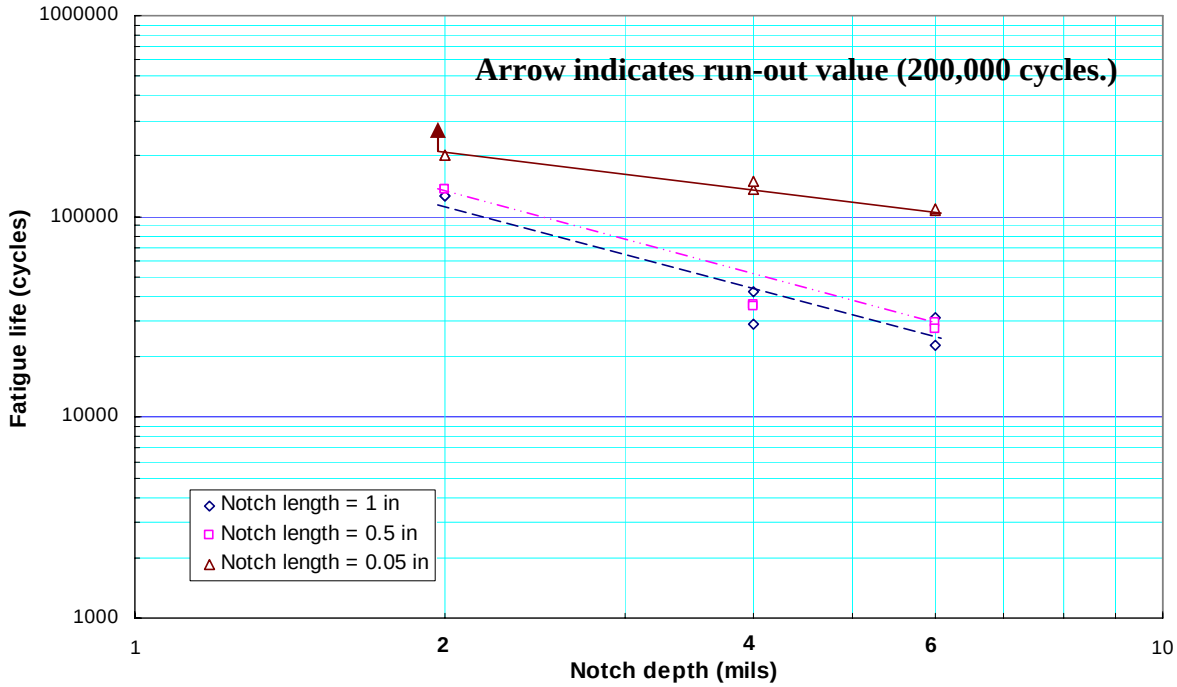

Figure 19 LMM notch depth versus fatigue life cycles to failure (1/2” OD × 0.043” TWT tubes).

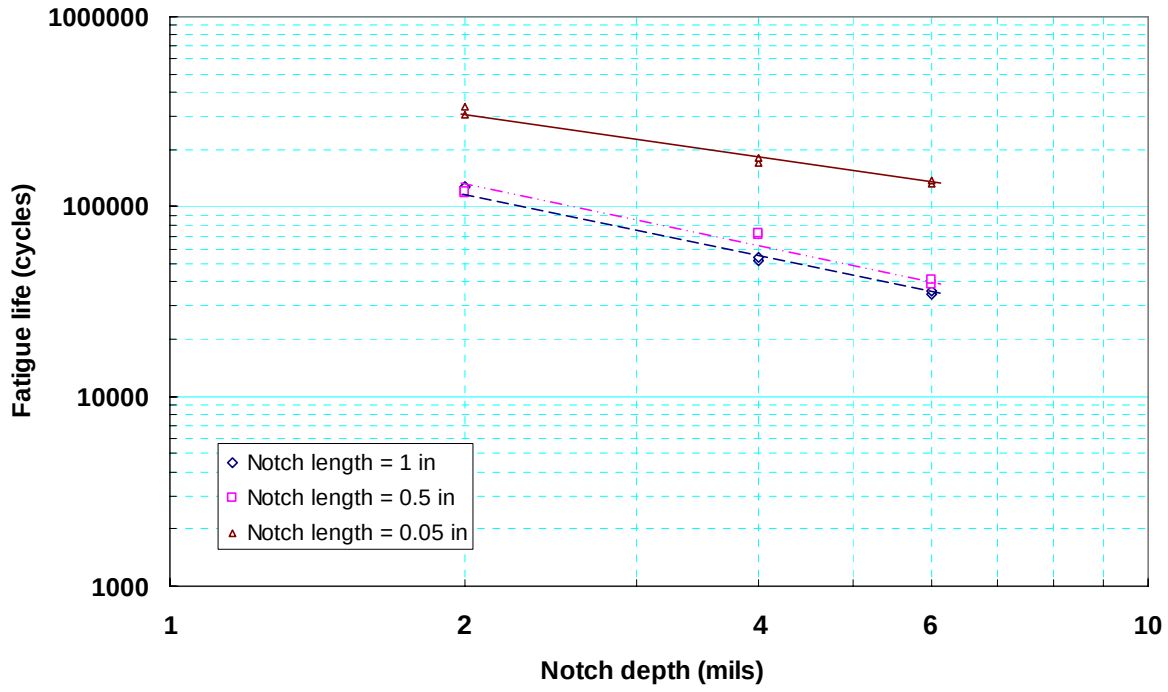

Figure 20 LMM notch depth versus fatigue life cycles to failure (5/8” OD × 0.054” TWT tubes).

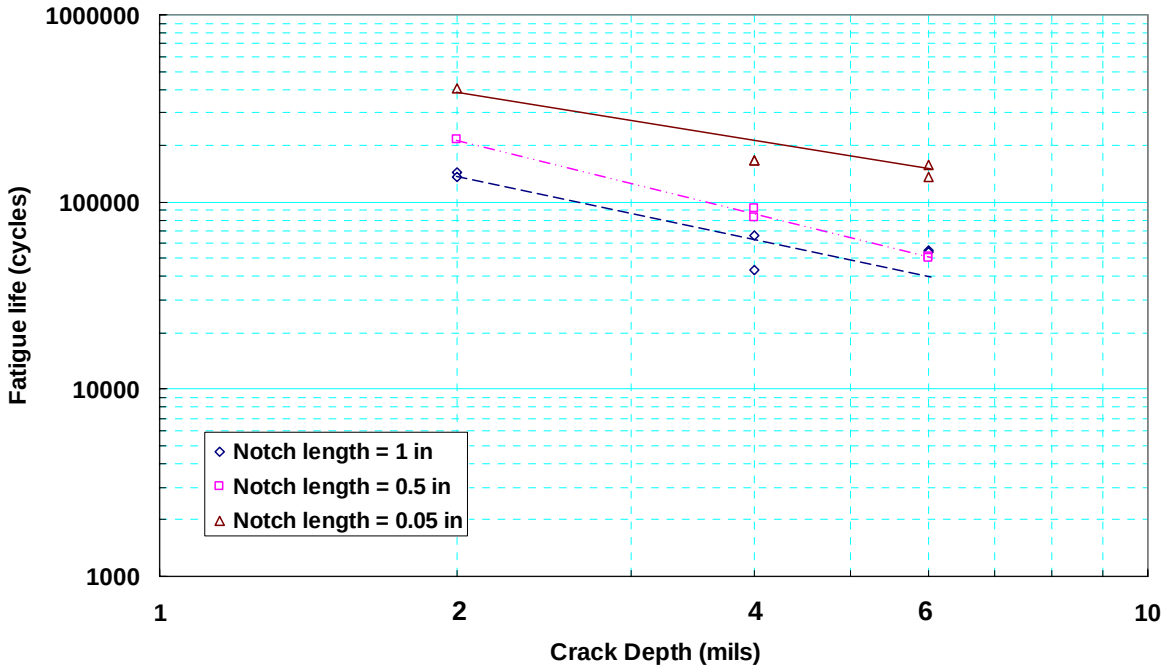

Figure 21 LMM notch depth versus fatigue life cycles to failure (3/4” OD × 0.065” TWT tubes).

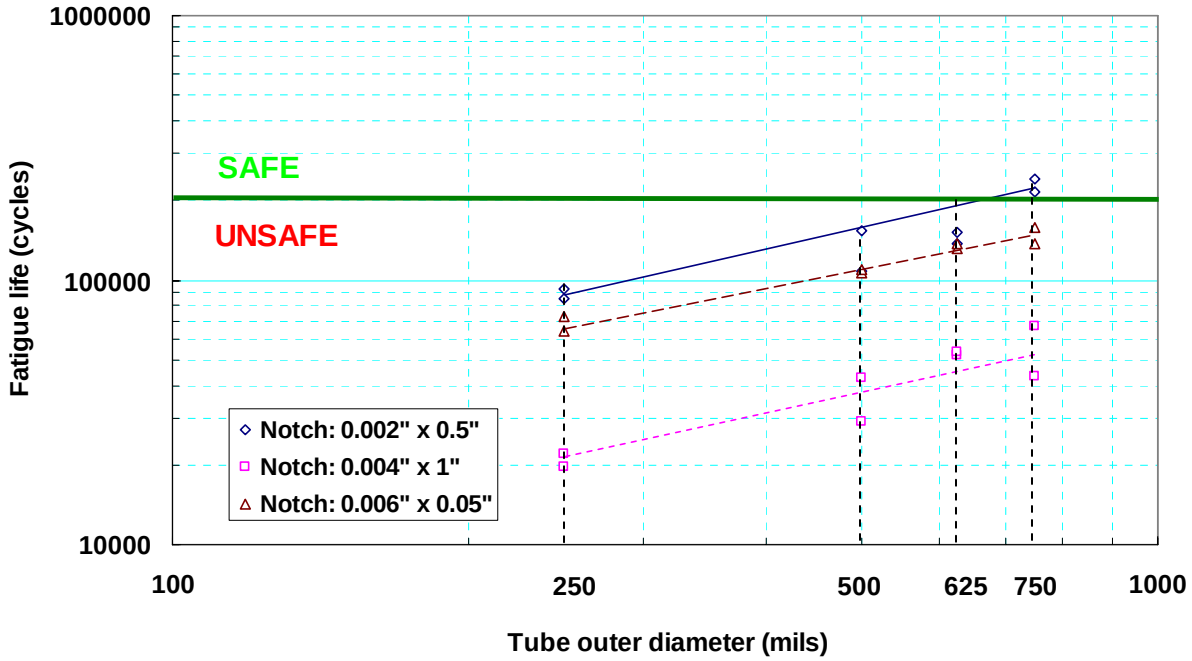

Figure 22 The fatigue life cycles to failure versus the tube outer diameter (OD).

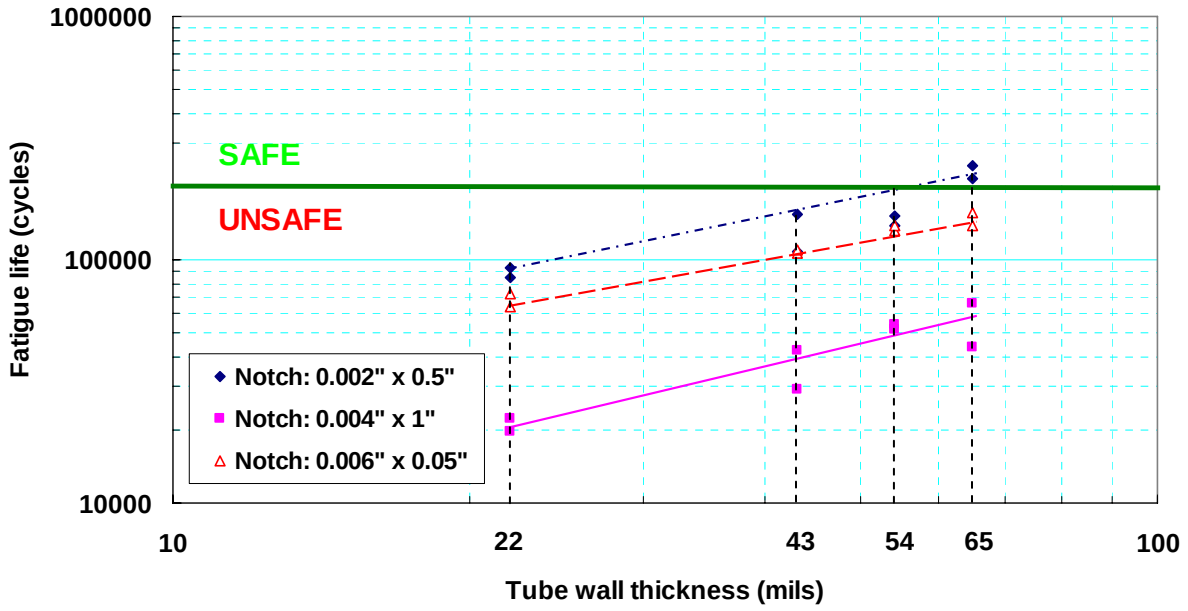

Figure 23 The fatigue life cycles to failure versus the tube wall thickness (TWT).

Table 1 Chemical composition of Ti-3Al-2.5V tube material [3]

Elements	Composition (wt %)
Al	2.990
B	<0.0005
C	0.005
Cu	<0.002
Fe	0.146
H	0.0014
Mn	0.001
N	0.002
O	0.091
Si	0.004
Ti	Bal.
V	2.500
W	<0.003
Y	<0.0005

Table 2 Laser micromachined notch dimensions for tubes of ¼" OD, 3/8" OD, ½" OD, 5/8" OD and ¾" OD.

Tube size	Notch depth	2mils				4mils				6mils			
	Notch length	0.02"	0.05"	0.5"	1"	0.02"	0.05"	0.5"	1"	0.02"	0.05"	0.5"	1"
¼"OD×0.022" TWT		√	√	√	√	√	√	√	√	√	√	√	√
½"OD×0.043" TWT		√	√	√	√	√	√	√	√	√	√	√	√
5/8"OD×0.054" TWT		-	√	√	√	-	√	√	√	-	√	√	√
¾"OD×0.065" TWT		-	√	√	√	-	√	√	√	-	√	√	√

Tube size	Notch depth	2mils				4mils		5mils			
	Notch length	0.025"	0.05"	1"	1.5"	0.025"	0.02"	0.025"	0.05"	1"	1.5"
3/8"OD×0.032" TWT		√	√	√	√	√	√	√	√	√	√

Tube size	Notch depth	7mils		9mils		
	Notch length	0.02"	0.025"	0.05"	1"	1.5"
3/8"OD×0.032" TWT		√	√	√	√	√

Notes: Mark " √ " denotes sample were prepared with the specified notch depth and length. Two samples were prepared for each combination of notch depth and length.

Table 3 Material properties of titanium alloy

Material data used in FEA models	
Modulus of elasticity, E, ksi	16,130
Poisson's ratio, ν	0.33
Yield strength (0.2% offset), σ_{ys}, ksi	118.1
Strength coefficient, K, ksi	150.9
Strain hardening exponent, n	0.0342
True fracture stress, σ_f, ksi	195.0
True fracture ductility, ε_f, in/in	0.55

Low cyclic fatigue data used in crack initiation life models	
Fatigue strength coefficient, σ_f', ksi	
Fatigue strength exponent, b	
Fatigue ductility coefficient, ε_f', in/in	
Fatigue ductility exponent, c	

Material data used in crack growth life model	
Paris crack growth rate constant, C,	3.00E-10
Paris exponent	4

Table 4 Inner pressure parameters used in impulse test program

Nominal pressure (psi)	Maximum pressure (psi)	Minimum pressure (psi)	Mean pressure (psi)
5,000	7,500	250	3,875

Table 5 Impulse pressure test results for the 1/4" OD ×0.022" TWT tubes

Specimen number	Tube size	Crack depth a_0 (inch)	Crack length $2c_0$ (inch)	Experimental life to failure (cycles)
1	¼" OD	0.002	0.020	> 200,000
2	¼" OD	0.002	0.020	> 200,000
3	¼" OD	0.002	0.050	> 200,000
4	¼" OD	0.002	0.050	> 200,000
5	¼" OD	0.002	0.5	84,887
6	¼" OD	0.002	0.5	92,583
7	¼" OD	0.002	1	64,058
8	¼" OD	0.002	1	77,527
9	¼" OD	0.004	0.020	> 200,000
10	¼" OD	0.004	0.020	> 200,000
11	¼" OD	0.004	0.050	98,466
12	¼" OD	0.004	0.050	107,162
13	¼" OD	0.004	0.5	28,437
14	¼" OD	0.004	0.5	31,193
15	¼" OD	0.004	1	19,798
16	¼" OD	0.004	1	22,137
17	¼" OD	0.006	0.020	> 200,000
18	¼" OD	0.006	0.020	> 200,000
19	¼" OD	0.006	0.050	63,768
20	¼" OD	0.006	0.050	72,340
21	¼" OD	0.006	0.5	9,203
22	¼" OD	0.006	0.5	10,857
23	¼" OD	0.006	1	2,560
24	¼" OD	0.006	1	3,164

Table 6 Impulse pressure test results for the 3/8" OD ×0.032" TWT tubes

Specimen number	Tube size	Crack depth a_0 (inch)	Crack length $2c_0$ (inch)	Experimental life to failure (cycles)
1	3/8" OD	0.002	0.025	> 200,000
2	3/8" OD	0.002	0.050	> 200,000
3	3/8" OD	0.002	1	182,412
4	3/8" OD	0.004	0.025	171,332
5	3/8" OD	0.005	0.020	> 200,000
6	3/8" OD	0.005	0.025	129,803
7	3/8" OD	0.005	0.050	127,786
8	3/8" OD	0.005	1	17,125
9	3/8" OD	0.005	1.5	18,023
10	3/8" OD	0.007	0.020	120,151
11	3/8" OD	0.009	0.025	46,890
12	3/8" OD	0.009	0.050	36,358
13	3/8" OD	0.009	1	2,300
14	3/8" OD	0.009	1.5	1,860

Table 7 Impulse pressure test results for the 1/2" OD ×0.043" TWT tubes

Specimen number	Tube size	Crack depth a_0 (inch)	Crack length $2c_0$ (inch)	Experimental life to failure (cycles)
1	½" OD	0.002	0.020	> 200,000
2	½" OD	0.002	0.020	> 200,000
3	½" OD	0.002	0.050	> 200,000
4	½" OD	0.002	0.050	> 200,000
5	½" OD	0.002	0.5	136,553
6	½" OD	0.002	0.5	136,933
7	½" OD	0.002	1	126,344
8	½" OD	0.002	1	299,083
9	½" OD	0.004	0.020	> 200,000
10	½" OD	0.004	0.020	> 200,000
11	½" OD	0.004	0.050	135,879
12	½" OD	0.004	0.050	149,134
13	½" OD	0.004	0.5	35,371
14	½" OD	0.004	0.5	36,194
15	½" OD	0.004	1	29,307
16	½" OD	0.004	1	42,370
17	½" OD	0.006	0.020	> 200,000
18	½" OD	0.006	0.020	> 200,000
19	½" OD	0.006	0.050	107,057
20	½" OD	0.006	0.050	109,117
21	½" OD	0.006	0.5	27,400
22	½" OD	0.006	0.5	29,557
23	½" OD	0.006	1	22,668
24	½" OD	0.006	1	31,068

Table 8 Impulse pressure test results for the 5/8" OD ×0.054" TWT tubes

Specimen number	Tube size	Crack depth a_0 (inch)	Crack length $2c_0$ (inch)	Experimental life to failure (cycles)
1	5/8" OD	0.002	0.050	307,792
2	5/8" OD	0.002	0.050	336,210
3	5/8" OD	0.002	0.5	117,225
4	5/8" OD	0.002	0.5	121,087
5	5/8" OD	0.002	1	126,344
6	5/8" OD	0.002	1	199,817
7	5/8" OD	0.004	0.050	170,274
8	5/8" OD	0.004	0.050	181,865
9	5/8" OD	0.004	0.5	71,076
10	5/8" OD	0.004	0.5	72,806
11	5/8" OD	0.004	1	51,669
12	5/8" OD	0.004	1	53,750
13	5/8" OD	0.006	0.050	132,102
14	5/8" OD	0.006	0.050	137,337
15	5/8" OD	0.006	0.5	38,885
16	5/8" OD	0.006	0.5	40,740
17	5/8" OD	0.006	1	34,656
18	5/8" OD	0.006	1	36,042

Table 9 Impulse pressure test results for the 3/4" OD ×0.065" TWT tubes

Specimen number	Tube size	Crack depth a_0 (inch)	Crack length $2c_0$ (inch)	Experimental life to failure (cycles)
1	¾" OD	0.002	0.050	403,163
2	¾" OD	0.002	0.050	403,581
3	¾" OD	0.002	0.5	215,954
4	¾" OD	0.002	0.5	242,444
5	¾" OD	0.002	1	137,298
6	¾" OD	0.002	1	144,086
7	¾" OD	0.004	0.050	167,876
8	¾" OD	0.004	0.050	168,114
9	¾" OD	0.004	0.5	83,172
10	¾" OD	0.004	0.5	92,287
11	¾" OD	0.004	1	43,377
12	¾" OD	0.004	1	66,504
13	¾" OD	0.006	0.050	137,093
14	¾" OD	0.006	0.050	157,003
15	¾" OD	0.006	0.5	50,223
16	¾" OD	0.006	0.5	50,667
17	¾" OD	0.006	1	53,716
18	¾" OD	0.006	1	54,774

Table 10 Comparison of the proposed and actual length and depth of the notches by LMM

Proposed depth & length	Actual depth & length (Sample 1)	Actual depth & length (Sample 2)
2 mil × 50 mil	1.94 mil × 52 mil	
2 mil × 1 inch	2.12 mil × 1.009 inch	
4 mil × 20 mil	3.88 mil × 21 mil	4.21 mil × 22 mil
4 mil × 50 mil	4.23 mil × 49 mil	
4 mil × 0.5 inch	3.96 mil × 0.508 inch	
6 mil × 50 mil	5.98 mil × 52 mil	6.22 mil × 53 mil
6 mil × 0.5 inch	6.07 mil × 0.490 inch	
6 mil × 1 inch	5.93 mil × 1.010 inch	6.27 mil × 1.012 inch

Table 11 Ti-tubing outer diameter variation data

Nominal OD inches	Tolerance, in plus	Tolerance, in minus
0.187>OD>0.093	0.002	0.000
0.499>OD>0.187	0.003	0.000
0.749>OD>0.499	0.004	0.000
0.999>OD>0.749	0.004	0.001

Nominal ID inches	Tolerance, in plus	Tolerance, in minus
0.338>OD>0.000	0.0015	0.0015
0.449>OD>0.338	0.002	0.002
0.673>OD>0.449	0.0025	0.0025
0.900>OD>0.673	0.003	0.003

DAAD-19-99-1-0277

NAVAIR PROJECT REPORT – Part II

Three-Dimensional Finite Element and Fracture Mechanics Study of Fatigue Damage Limits for Straight Titanium Tubes used in V-22 Osprey Tilt-rotor Aircraft

Kan Ni and Mool C. Gupta
University of Virginia

Submitted to
Mr. Kevin Woodland
V22 Program Office
Patuxent River, MD 20670

Principal Investigator: Prof. Mool C. Gupta
Department of Electrical & Computer Engineering,
University of Virginia,
Charlottesville, Virginia 22904,
Email: mgupta@virginia.edu,
Phone: 757-325-6850
Fax: 757-325-6988

May 15, 2007

Executive Summary

A systemized methodology of three-dimensional (3D) finite element (FE) modeling and computational fracture mechanics analysis has been established for the study of fatigue damage limit of straight titanium tubes used in V-22 tilt-rotor aircraft. A laser micromachining technology is developed and it provides sharp notch in the specimen, therefore only crack growth stage is considered herein. Totally five different outside diameter (OD) tube of different wall thickness (TWT) are studied, including 3/8 inch OD with 0.032 inch TWT, 1/4 inch OD with 0.022 TWT, 1/2 inch OD with 0.043 inch TWT, 5/8 inch OD with 0.054 inch TWT, and 3/4 inch OD and 0.065 inch TWT, respectively. The J-integral and stress intensity factors (SIF) are calculated from 3D FE models for different sizes of initial cracks on the outside surface of Ti tubes. Those cracks are modeled as longitudinal surface cracks with different aspect ratios which cover a very wide range from 0.5 to 0.0001, i.e. from normal cracks to very long cracks. The very long crack is studied with 3D FE for the first time to the authors' knowledge. Fatigue crack propagation lives are also calculated for all tubes. In the end, the fatigue damage limits of Ti tubes are established. The 3D FE results of J-integral and SIF agree well with NASGRO results while NASGRO only consider a limited range of aspect ratios. The modeling results of fatigue crack life also agree well with experimental results. It shows that the novel methodology developed can be applied to obtain damage limit curves for tubes of various diameter and wall thickness. This was a successful collaborative effort between the researchers at the University of Virginia, V-22 program office, NAVAIR materials testing and hydraulics testing laboratories.

1, Introduction

It is well known that fatigue crack initiation and propagation is the most critical failure mode in aircraft. Consequently, damage tolerance and durability design has played a predominant role in modern aircraft structures design against fatigue and fracture. The basic idea of damage tolerance design is that there exists inevitable initial fatigue damage and cracks in structure components before or during the service, and one of the basic targets is to make accurate prediction of the fatigue crack initiation and propagation life for structures.

Surface flaws such as gouges, scratches, fretting, dents, and pits, have been observed on the outer surface of in-service titanium tubes in V-22 tilt-rotor aircraft as indicated in Figure 24 [1]. Assessment of allowable fatigue damage of in-service tubes is therefore important to avoid fatigue failure and sustain the aircraft for long-term operation. The focus of the establishment of damage limits for titanium tubes is to ensure the safety of the aircraft and provide an efficient methodology to determine if the tube should be replaced in the aircraft if a damage is noted.

During the last three years, in this project, damage limit curves have been developed by using finite element analysis and laboratory testing to determine what defect depth and length are acceptable to avoid hydraulic leak failure within required service hours. The strategies to determine the damage limit curves are:

1) identify the worst type of flaw that makes a tube experience the shortest fatigue life to failure;
2) conduct internal impulse pressure tests for the tubes with the worst type of flaw with different flaw profiles (i.e., combination of flaw depth and length) to obtain the relationship between the flaw profile and fatigue life;
3) determine stress and strain distributions around the worst type of flaw when the tube is subjected to inner impulse pressures used in the tests;
4) make fatigue life prediction of the tube based on the predicted stresses and strains and validate the predicted life with experimental data; and
5) determine the flaw profile of the tube that can resist $\geq$200,000 cycle internal impulse pressure and generate the damage limit curve for the tube. Life cycle of 200,000 dynamic pressure levels is assumed to correspond to about 10,000 hours of flight time.

In a V-22 aircraft, there are a variety of tube geometries (i.e., outer diameters (OD) and tube wall thicknesses (TWT)), profiles (straight tubes and bend tubes with different bent angles), and surface flaws (gouge, scratch, dent, fretting, pits) under different hydraulic pressure levels. The challenge the project team faced was that it was impossible to perform impulse pressure tests and experimentally determine fatigue lives to failure for the tubes within two years with the available funding. Finite element (FF) modeling, therefore, played a fundamental role in the project as it could cover all sizes of tubes with all types of detected defects. FE modeling has been applied to determine stress and strain distribution, to predict fatigue life, and to validate testing results. In the first phase of the project, the five strategies introduced aforementioned were applied to the straight tube with 3/8”OD and 0.032” TWT. Later from last year till now, the damage limit

curves for tubes with 1/4" OD and 0.022" TWT, 1/2" OD and 0.043" TWT, 5/8" OD and 0.054" TWT, and 3/4" OD and 0.065" TWT also have been experimentally determined.

2, Background

There are three major methodologies in current fatigue life prediction, i.e., stress-based (S-N curve) method, strain-based (ε-N curve) method, and fracture mechanics. While ε-N curve method is used in the fatigue crack initiation stage, and fracture mechanics is used in the crack propagation stage. The total fatigue life is the sum of loading cycles applied in the two stages of crack initiation and propagation.

There are two key points in fracture mechanics, the first is the calculation of stress intensity factor (SIF) and J-integral, the second is the calculation of crack propagation. For real structural components due to the complexity in the geometry, boundary and loading conditions, the two key points above can be resolved numerically only. Thus computational fracture mechanics plays a significant role.

In computational fracture mechanics, the calculation of SIF and J-integral is the fundamental problem. There are three major methods, the finite element method, the boundary element method, and the meshless method, while in the meshless method the 3D resolution is still under development.

Generally, finite element methods in computational fracture mechanics can be divided into three categories: the stress and displacement correlation method, the modified crack closure integral method, and the J-integral method by the equivalent domain integral.

Barsoum (1974) proposed a stress and displacement matching method.

Shih et al. (1976) proposed an energy domain integral methodology. Atluri (1982), Nikishkov and Atluri (1987) proposed an equivalent domain integral method for mixed mode 3D calculations.

Ribicki and Kanninen (1977), Raju (1987), proposed the modified crack closure integral method, respectively.

Parks (1974) and Hellen (1975) proposed a virtual crack extension approach independently. Later, deLorenzi (1982, 1985) improved this method from finite element to continuum, and obtained a general expression of the energy release rate in 3D problems.

MSC/MARC uses the J-integral in calculating the energy release rate. And the J-integral is based on the virtual crack extension approach proposed by deLorenzi (1982, 1985).

In this project, we adopt MSC/MARC to perform all the J-integral calculations for all tube with different sizes and aspect ratios.

Newman and Raju (1976, 1982) calculated stress intensity factors for a wide range of semi-elliptical longitudinally surface cracks on the inside and outside of a cylinder. All of their results have been curve-fitted and embedded in NASGRO. The FE method which Newman and Raju used belongs to the stress and displacement matching method.

However, for surface crack in NASGRO, the aspect ratio (crack depth to surface half-length a/c) ranges from 0.1 to 1.2. Moreover, Newman also made a linearization assumption in which the stress distribution across the vessel wall was assumed as a straight line connecting the stresses on the internal and external surface.

Lin and Smith (1997) set up a step by step numerical analysis methodology for fatigue crack growth of external surface crack in pressurized cylinders. They also used the 1/4 point displacement methods (Barsoum, 1974) to calculate the stress intensity factors. Their step by step multiple degrees of freedom model permits the direct prediction for the shape of propagating crack. However, only two aspect ratios, a/c=0.2 and a/c=1 were considered in their calculation.

In this project, the aspect ratio of external surface crack in all Ti tubes ranges from 0.004 to 0.5, therefore it is necessary to develop a new 3D FE model for the numerical fracture mechanics analysis of surface cracks in internal pressurized Ti tubes.

The principle task in this study is firstly to develop a new 3D FE model by applying MSC/MARC to calculate the J-integral and stress intensity factors; the second is to predict the fatigue life of surface crack growth. The whole flowchart is as follows:

1) 3D FE meshing of tube, sub meshing of crack area;
2) Loading and boundary conditions;
3) Stress/strain analysis;
4) J-integral calculation;
5) Stress intensity factor calculation;
6) Fatigue crack initiation life prediction;
7) Fatigue crack propagation life prediction;
8) Damage limit analysis;
9) Validation and verification;
10) Considering different sizes of tubes.

The 3D FE model of 3/8” OD and 0.032” TWT tube was established first. Then this FE model was used to study the other tubes by just changing geometrical parameters.

In this project, the laser micro-machining (LMM) is applied to make the pre-crack in Ti tubes. Compared with the electrical discharge machining (EDM) which produces blunt notch root, LMM can make initial cracks sharp enough in the Ti tube specimens, see Figure 25. As a result, the crack initiation life in all Ti tube specimens is very short thus can by neglected. Hence the crack propagation life of tube specimen becomes the focus of our study.

In Figure 25, one also can observe that the heat affected zone (HAZ) in LMM specimen is much smaller than HAZ in EDM specimen. Therefore, in this study, the effect of the residual stress in HAZ can be neglected for crack propagation in LMM specimens.

3, 3D Finite Element Calculation of the J-integral and Stress Intensity Factors

Recently, the numerical calculation of J-integral and stress intensity factor has been widely adopted, because this is only way available for fracture mechanics analysis of real structural components due to complexity in geometry and loading conditions.

The J-integral is defined by Rice (1968) as follows:

$$J = \int_{\Gamma} \left(W n_1 - T_i \frac{\partial u_i}{\partial x_i} \right) ds \tag{1}$$

where W is the strain energy density, T_i is the components of the traction vector, u_i is the displacement vector component, and ds is the length along an arbitrary contour Γ enclosing the crack tip in a counter-clock wise.

Moreover, stress intensity factors can be calculated from the J-integral in the following relationship:

$$J = \frac{1}{E'} \left(K_I^2 + K_{II}^2 \right) + \frac{\nu}{E} K_{III}^2 \tag{2}$$

in which K_I, K_{II} and K_{III} are the stress intensity factors for fracture modes I, II, and III respectively, $E' = E$ for plane stress and $E' = E/(1-\nu^2)$ for plane strain, E is the elastic modulus and ν is the Poisson's ratio, respectively.

deLorenzi (1982), derived a general expression (3D) for the energy release rate as follows

$$G = \frac{1}{A_c} \int_V \left\{ \left(\sigma_{ij} \frac{\partial u_j}{\partial x_k} - W \delta_{ik} \right) \frac{\partial \Delta x_k}{\partial x_i} - f_i \frac{\partial u_i}{\partial x_j} \Delta x_j \right\} dv - \frac{1}{A_c} \int_S t_i \frac{\partial u_i}{\partial x_j} \Delta x_j \, ds \tag{3}$$

where A_c is the increase in cracked area produced by the virtual crack extension, V is the volume and S the surface of the cracked body, σ_{ij} the stress tensor, u_i the displacement vector, W the strain energy density, f_i the body force vector, t_i the surface tractor vector, δ_{ij} Kronecker's delta, and Δx_j is a mapping function which maps the body containing the crack into a body with a slightly increased crack length.

MSC/MARC employs the deLorenzi definition in Eq. (3) to calculate the J-integral, and is termed as Lorenzi option. This method is advantageous to use so-called quarter point element at the crack tip which is adopted in ABAQUS and ANSYS. Moreover, this method is also much more convenient than ABAQUS and ANSYS, especially in the meshing stage of the FE modeling around the crack tip.

Because the numerical calculation of J-integral or energy release rate is very time-consuming, the sub-modeling technique has to be used in ABAQUS and ANSYS. First, the FE modeling without crack is set up and the stress and displacement is obtained, then a new FE modeling with crack is established and the previous displacement field is imposed in the sub-model of the crack.

The advantage of using MSC/MARC is that the sub-modeling technique is no longer needed. The advanced contact technique is used herein and only one time is needed to perform the FE calculation.

4, Fatigue Crack Growth Rate and Crack Propagation Life Prediction

When a structural component is subjected to a fluctuating loading which is of either constant or variable amplitude, the crack will propagate if the stress intensity factor range exceeds the threshold of stress intensity factor range.

Paris law is the well known crack growth rate:

$$\frac{da}{dN} = C(\Delta K)^n \tag{4}$$

where a is the crack length, N the number of loading cycles to failure, ΔK the stress intensity factor range, C the growth rate coefficient, and n the growth rate exponent.

Another one is Walker's law under which stress ratio is taken into consideration:

$$\frac{da}{dN} = C[(1-R)^q \Delta K]^m, \qquad R \geq 0 \tag{5}$$

where $R = S_{\min} / S_{\max}$ is the stress ratio, q and m are growth rate exponents. Obviously, when $R = 0$, Walker's law becomes Paris law.

The NASGRO equation of crack growth rate takes both fatigue crack closure and rapid crack growth effects into consideration:

$$\frac{da}{dN} = C\left[\left(\frac{1-f}{1-R}\right)\Delta K\right]^n \frac{\left(1-\Delta K_{th}/\Delta K\right)^p}{\left(1-K_{\max}/K_c\right)^q} \tag{6}$$

where a is the crack depth, N is crack growth life cycles, C, n, p, and q are empirically derived material constants, R is the stress ratio, ΔK is the SIF range, $K_{\max}$ is maximum SIF, and K_c is fracture toughness. The crack opening function f was defined by Newman (1984). The formulas of calculating f and ΔK_{th} were presented by Forman et al. (2004).

Numerically integrating a selected crack growth rate law described above, the fatigue crack growth life under both constant and variable amplitude loading can be predicted.

5, 3D Finite Element Modeling and Results

5.1, 3D FE modeling

The internally pressured Ti tube with outer surface crack is depicted in Figure 26.a and 26.b. Due to symmetry in geometry and loading, only one quarter of the tube is modeled by using the 3D FE method.

The tube of 3/8" OD and 0.032" TWT tube was modeled in 3D FE first. The nominal internally pressure is 5,000 psi, the material property parameters are listed in Table 12.

Firstly, the 3D FE analysis is performed for a tube without any surface crack, the FE modeling with loading and boundary conditions, and the stress results are presented in Figure 27.a and 27.b. It is shown that without any crack, the stress distribution in the tube decreases slowly from the inside to outside surface along the thickness directions.

When the surface crack exists on the outside surface in tubes, the 3D FE modeling especially the meshing details around the crack tip and the stress distribution are presented in Figure 28.a, 28.b, 28.c, and 28.d. Figure 28.a and 28.b are two different meshing models around the crack tip. However, the calculated stress distribution and the J-integral are nearly the same as shown in Figure 28.c and 28.d. There is an obviously stress concentration strip along the crack tip.

5.2, 3D FE Calculation of J-integral and Stress Intensity Factors

Once the 3D FE modeling is established for the 3/8" OD and 0.032" TWT tube with an outer surface crack, it is easy to change the crack length and width which are treated as basic parameters inputted in to the MSC/MARC commands program. Consequently, a series of 3D FE results are obtained for different surface depth.

Figure 29.a and 29.b depict the 3D stress results along the crack tip for 3/8" OD and 0.032" TWT tube at different initial crack depths, a_0=0.009" and 0.015", respectively, the aspect ratio of the crack depth to crack length a/c=0.25. In fact, a wide range of the aspect ratio has been considered and calculated in this study.

Figure 30 depicts the comparison between the present 3D FE calculated results of the stress intensity factor and that of NASGRO (Forman et al. 2004), while the aspect ratio is 0.25. It can be seen that they agree with each well. However, NASGRO only can consider the aspect ratio within the range of between 0.1 and 1.2. But the present 3D FE model developed herein can consider a wide range of the aspect ratio.

5.3, Numerical Prediction of Fatigue Crack Propagation Life of 3/8" Tubes

Both the Paris law and the NASGRO equation are chosen respectively in the prediction of crack propagation life of 3/8" Tubes. The material property parameters are determined with reference to the NASGRO date base, as shown in Figure 31. When Walker's law and Paris law are used to predict the fatigue crack growth life, the only different parameter is $n = 4.5$ instead of $n = 4$.

The fluctuating fatigue loading for all tube specimens is schematically presented in Figure 32. Where Nominal pressure is 5,000 psi, the maximum pressure is 7,500 psi, the minimum pressure is 250 psi, and the mean pressure is 3,875 psi.

Although theoretically the present 3D FE modeling can consider different aspect ratios, the step by step numerical method proposed by Lin and Smith (1997) is not adopted herein in the prediction of crack propagation. Because it needs more than hundreds steps of FE remodeling, especially re-meshing along the crack tip for any tube at a given initial value of aspect ratio, and we only have a limited time to finish all 3D FE modeling for all tubers at a large variety of different sizes. Therefore, the constant aspect ratio assumption is made herein in the prediction of crack growth which means only the worst case is taken into consideration and this will produces a relatively conservative result.

Table 13 and Figure 33 present the 3D FE modeling result of the crack growth life compared with experimental results, for two aspect ratios of a/c=0.25 and 0.5, at three fatigue loading levels at which the nominal pressure is 4,500 psi, 5, 000 psi, and 5, 500 psi, respectively. It shows that the modeling prediction agrees well with the experimental results.

5.4, Numerical Prediction of Fatigue Crack Propagation Life of Different Tube Diameter

Similar to 3/8" tubes, the 3D FE modeling results of fatigue crack prediction of other size tubes are also calculated.

Table 14 presents the modeling prediction compared with experimental results for1/4" tubes, Table 15 presents the modeling prediction compared with experimental results for1/2" tubes,

Table 16 presents the modeling prediction compared with experimental results for5/8" tubes, Table 17 presents the modeling prediction compared with experimental results for3/4" tubes.

Table 18 presents the modeling prediction compared with recently obtained new experimental results for 3/8" tubes with a series of different crack depths and aspect ratios.

It can be seen that for all tubes in all cases, the 3D FE modeling prediction agree well with experimental results. Among all cases, with the same crack depth and aspect ratio, 1/4" tube has the shortest life.

5.5, 3D FE Modeling of Median Size Crack

In all literatures, the surface crack in the internally pressured tube is treated as being of semi-elliptical configuration at an aspect ratio of $0.1 \leq a/c \leq 1.2$. However, when $a/c \leq 0.2$, the initial crack produced by LMM is no longer of semi-elliptical shape. The bottom of most of the crack tip is a straight line as shown in Figure 34.a. Herein it is called as median size crack and is modeled by 3D FE as presented in Figure 34.b. The stress distribution is shown in Figure 34.c.

The J-integral and stress intensity factor obtained in this 3D FE modeling are a little lower than those of the semi-elliptical 3D FE modeling. Because the time is limited, the result of 3D FE modeling of median size cracks is not presented here in detail.

5.6, 3D FE Modeling of Very Long Crack

In this study, the scratch on the external surface of internally pressured tubes is treated as being the most critical initial damage, and modeled as surface crack. In practical situation, some scratch is very long along the longitudinal direction of tubes. And the corresponding aspect ratio is very large than the general case such as that considered in NASGRO. So it is very important to establish the 3D FE modeling of so called very long surface crack on the outside surface of tubes.

One alternative way is to simplify the 3D very long crack as 2D problem. This will ignore the aspect ratio effect, and all long cracks with different aspect ratios will be treated as a same 2D crack. Obviously, this will produce a relatively conservative prediction of crack growth life.

For very long crack, the J-integral as well as the stress intensity factors along the crack tip vary slowly in the middle part, but rapidly in the two ends of the crack. The J-integral takes the maximum value in the middle point in the crack depth direction, and takes relatively low values in the two ends of the crack. Therefore, in the experiment, the bottom of the long crack tip grows firstly and quickly, there is nearly no crack growth that can be observed in the two ends of the long crack.

The step by step method proposed by Lin and Smith seems the ideal one to model the very long crack growth. However, the re-meshing of the crack tip is very tedious and time consuming. Due

to the limited time, in this study, a simplified 3D FE modeling of very long cracks are established, as shown in Figure 35.

Figure 36 depicts the 3D FE modeling of very long crack in 1/4" tubes, Figure 37 depicts the 3D FE modeling of very long crack in 1/2" tubes, Figure 38 depicts the 3D FE modeling of very long crack in 5/8" tubes, and Figure 39 depicts the 3D FE modeling of very long crack in 3/4" tubes.

The predicted results of very long crack growth life compared with experimental results is presented in Table 19, 20, 21 and 22. Again, it can be seen that the predictions agree well with the experimental results, and 1/4" tubes are the critical one owing the shortest crack growth life for the same prescribed initial crack.

6, Conclusions

An accurate 3D FE model is developed for fracture mechanics (J-integral and stress intensity factor K) calculation of longitudinal surface cracks on the outside surface in internally pressured Ti tubes using MSC/Marc.

The 3D FE methodology developed herein can establish easily the geometry and meshing models of tubes with a wide range of aspect ratios. The advanced contact option is adopted to input the fine mesh around the crack tip into the globe FE mesh of tubes.

An efficient methodology is developed to predict fatigue crack propagation life of Ti tubes. The 1/4 tube has the shortest crack growth life when all tubes have the same crack depths and aspect ratios.

Normal crack, median crack, and long crack and their propagation life have been modeled successfully. Because the project time is limited, the step by step method proposed by Lin and Smith (1997) is not adopted herein. Instead it is assumed that the aspect ratio will not change when the crack grows.

Predictions of fatigue crack growth life agree very well with experimental results, especially it should be noted that the testing sampling for each case is very small.

7, Suggested Future Work

To develop an efficient step by step re-meshing technology for the real simulation of the surface crack growth, especially for the very long crack growth.

To develop an elastic-plastic 3D FE modeling for the very long cracks and its growth.

The present 3D FE methodology can be easily used for bent tubes.

REFERENCES

Pregger, Bruce, 2004, "Titanium Tube Investigation – In-Service Tube Damage,"
1. Presentation by NAVAIR Material, March 23, 2004, Applied Research Center, Old Dominion University.

Atluri SN, Path-independent integrals in finite elasticity and inelasticity, with body forces, inertia, and arbitrary crack-face conditions, *Engineering Fracture Mechanics*, v 16, n 3, 1982, p 341-64

Barsoum, RS, Application of quadratic isoparametric finite elements in linear fracture mechanics, *International Journal of Fracture*, v 10, n 4, Dec. 1974, p 603-5

de Lorenzi, HG, On the energy release rate and the J-integral for 3-D crack configurations, *International Journal of Fracture*, v 19, n 3, July 1982, p 183-93

de Lorenzi, HG, Energy release rate calculations by the finite element method, *Engineering Fracture Mechanics*, v 21, n 1, 1985, p 129-43

Hellen, T. K.; Blackburn, W. S. Calculation of stress intensity factors for combined tensile and shear loading, *International Journal of Fracture*, v 11, n 4, Aug, 1975, p 605-617

Nikishkov, G.P, Atluri, S.N. Calculation of fracture mechanics parameters for an arbitrary three-dimensional crack, by the `equivalent domain integral' method
Source: *International Journal for Numerical Methods in Engineering*, v 24, n 9, Sept. 1987, p 1801-21

Parks, D.M, A stiffness derivative finite element technique for determination of crack tip stress intensity factors, *International Journal of Fracture*, v 10, n 4, Dec. 1974, p 487-502

Raju, I.S, Calculation of strain-energy release rates with higher order and singular finite elements, *Engineering Fracture Mechanics*, v 28, n 3, 1987, p 251-74

Rybicki, E.F, A finite element calculation of stress intensity factors by a modified crack closure integral, *Engineering Fracture Mechanics*, v 9, n 4, 1977, p 931-8

Shih CF, deLorenzi HG, German MD, 1976, Crack extension model with singular quadratic isoparametric element, International Journal of Fracture, 12 (4): 647-651

Newman, JC. 1976, Fracture analysis of surface and through cracks in cylindrical pressure vessels, NASA Technical Note, NASA TN D-8352
Raju, I. S. and Newman, J. C., 1982, "Stress-Intensity Factors for Internal and External Surface Cracks in Cylindrical Vessels," *Journal of Pressure Vessel Technology*, Vol. 104, pp. 293-298.

Rice, J. 1968, A path-independent integral and approximate analysis. of strain concentrations by notches and cracks. J. AppL Mech. 35: 379-386

Paris, P. C. and Erdogan, F. (1963) A critical analysis of crack propagation laws. *Trans. ASME J. Basic Engng*. 85, 528–534.

Walker, K. (1970) The effect of stress ratio during crack propagation and fatigue life for 2024-T3 and 7075-T6 aluminum. ASTM STP 462, pp. 1–14.

Newman JC. A crack opening stress equation for fatigue crack growth. International Journal of Fracture 1984; 24:131-135.

Forman RG, Shivakumar V, Mettu SR, Newman JC. Fatigue crack growth computer program NASGRO Version 4.1; reference manual 2004.

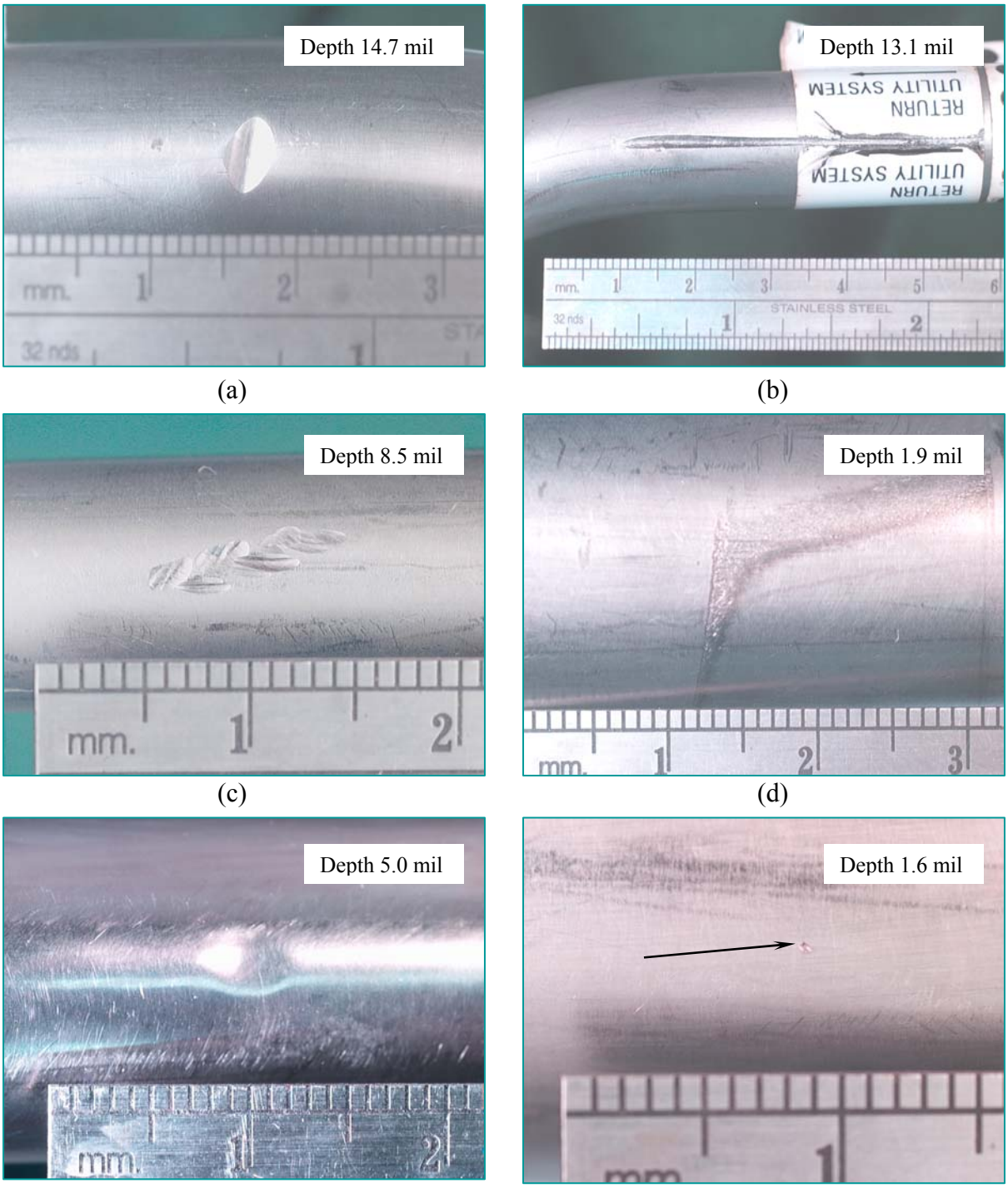

(a) (b)

(c) (d)

(e) (f)

Figure 24 In-service titanium tube damages: (a) Gouge; (b) Scratch; (c) Abrasion; (d) Fretting; (e) Dent; and (f) Pit (copied from [Reference 1]).

Figure 25.a EDM notch, depth=0.009”, width=0.006”

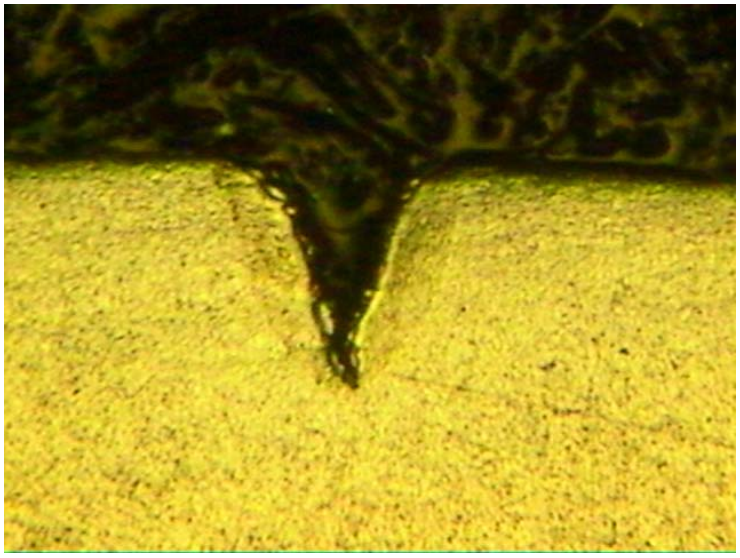

Figure 25.b LMM notch, depth=0.009”

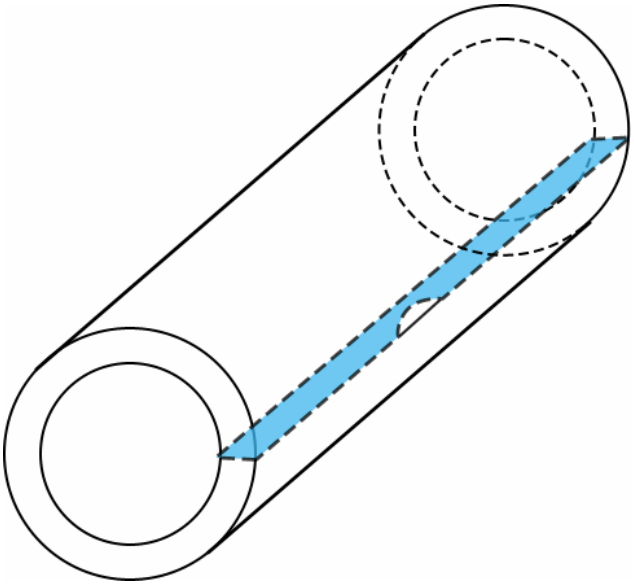

Figure 26.a Internally pressured tube with outer surface crack

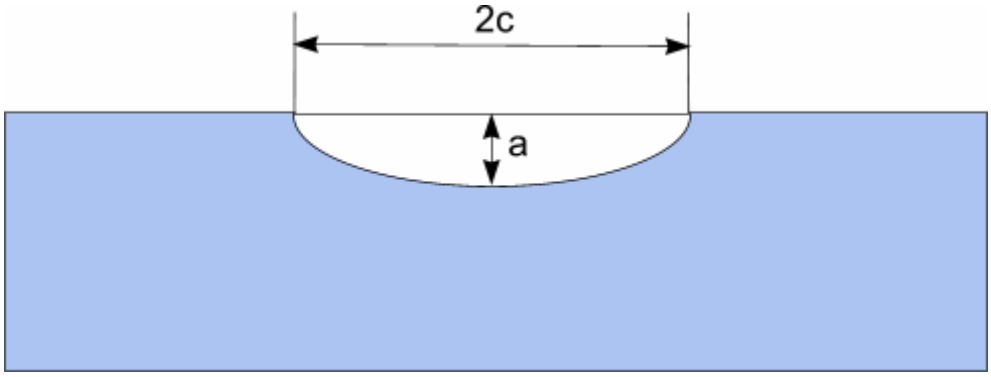

Figure 26.b, outer surface crack

Table 12, Material properties of Ti tubes

Modulus of elasticity, E, ksi	16,130
Poisson's ratio, ν	0.33
Yield strength (0.2% offset), σ_{ys}, ksi	118.1
Strength coefficient, K, ksi	150.9
Strain hardening exponent, n	0.0342
True fracture stress, σ_f, ksi	195.0
True fracture ductility, ε_f, in/in	0.55

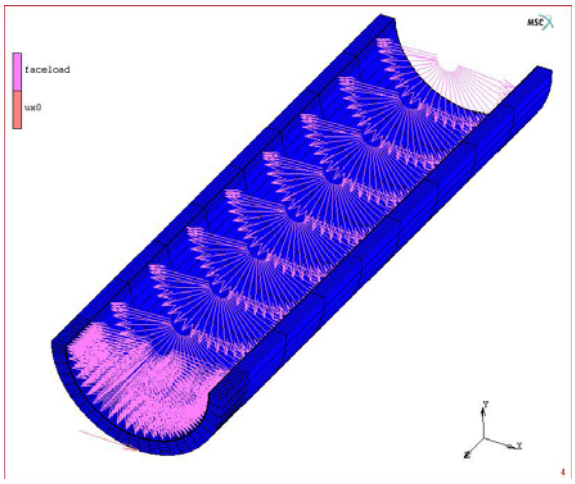

Figure 27.a, 3D FE modeling with loading and boundary conditions

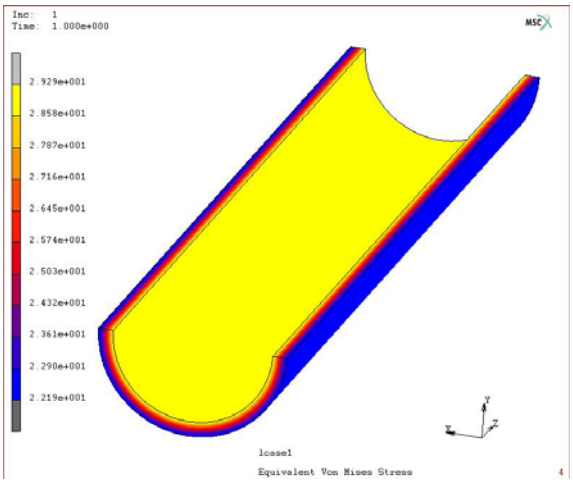

Figure 27.b, 3D FE stress without crack

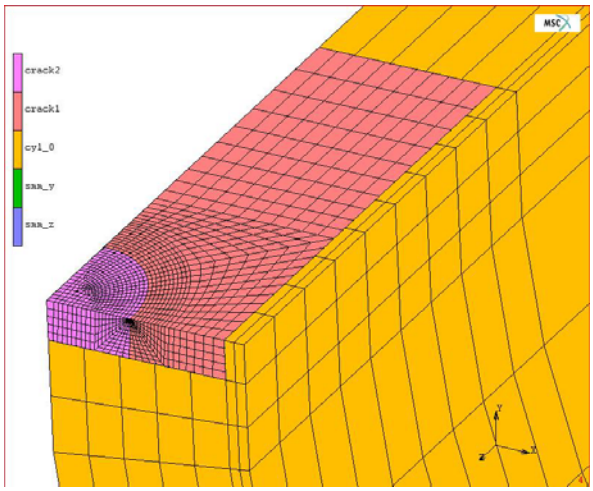

Figure 28.a, 3D FE meshing 1

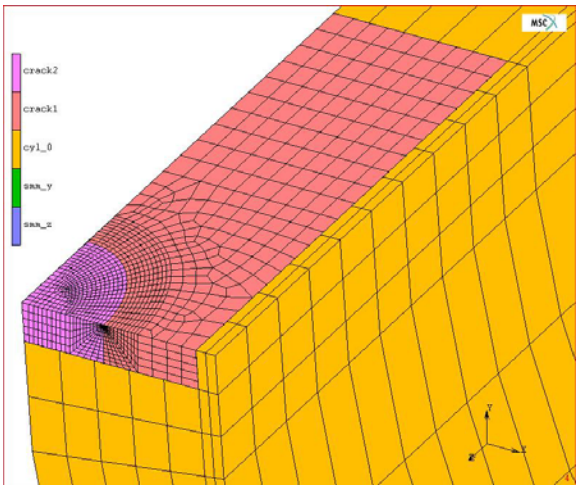

Figure 28.b, 3D FE meshing 2

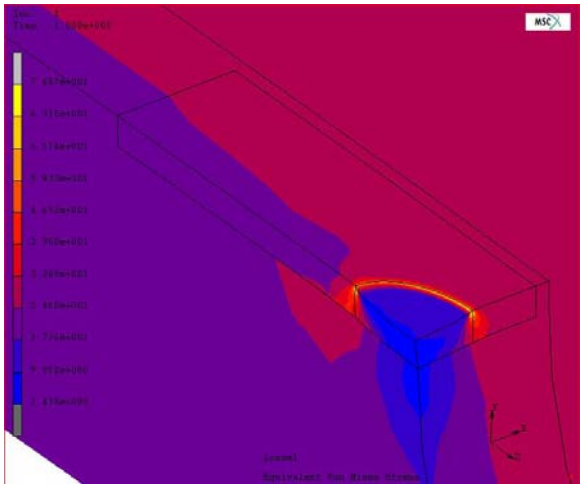

Figure 28.c, Stress distribution around crack

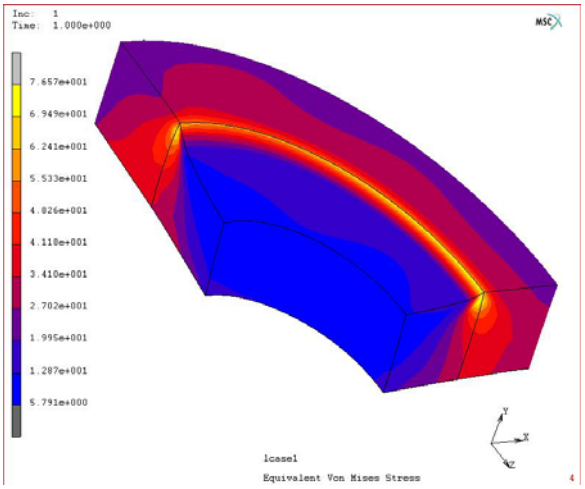

Figure 28.d Stress around crack tip

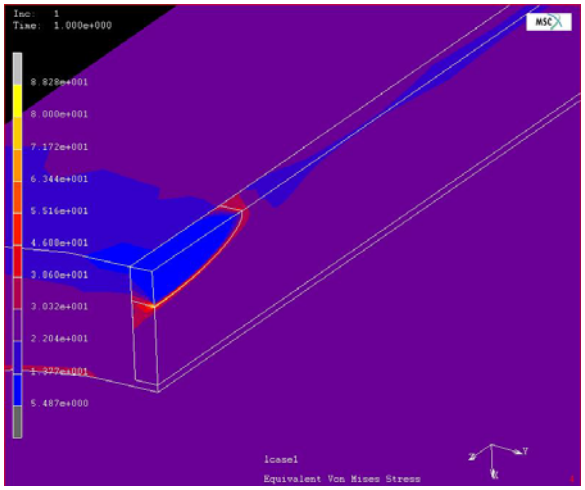

Figure 29.a, a_0 =0.009", a/c=0.25

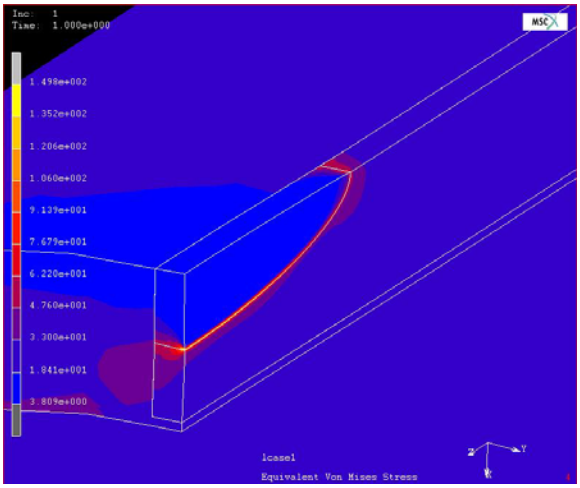

Figure 29.b, a_0 =0.015", a/c=0.25

.

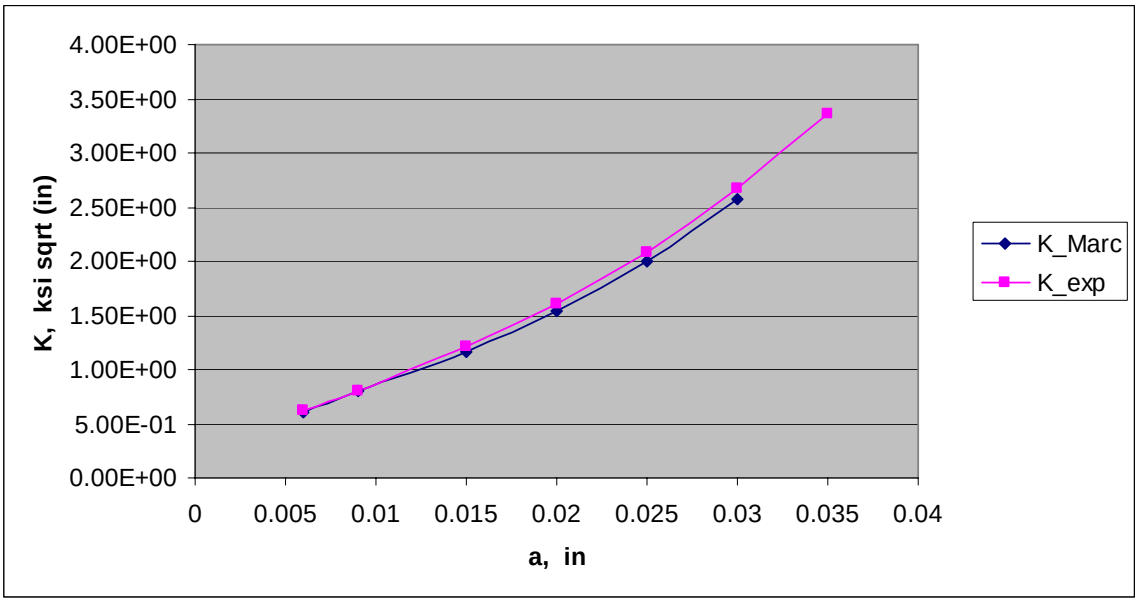

Figure 30, the 3D FE stress intensity factor compared with NASGRO

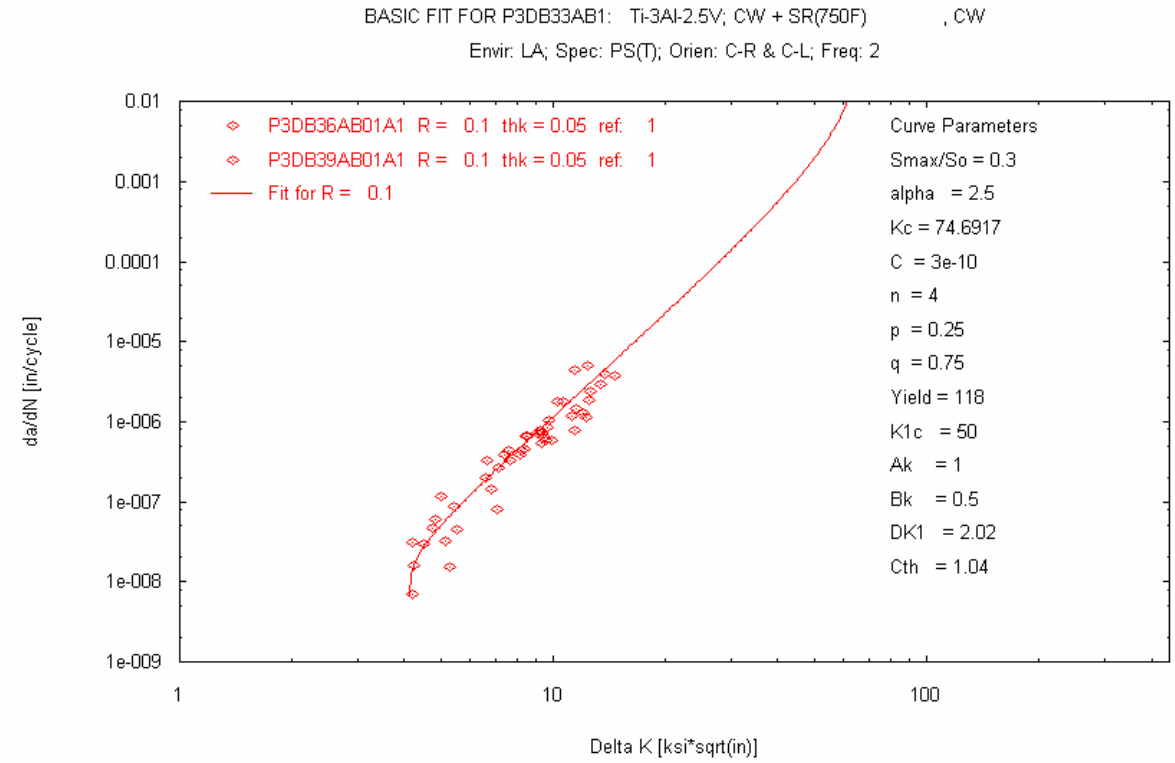

Figure 31, Crack growth rate and related parameters

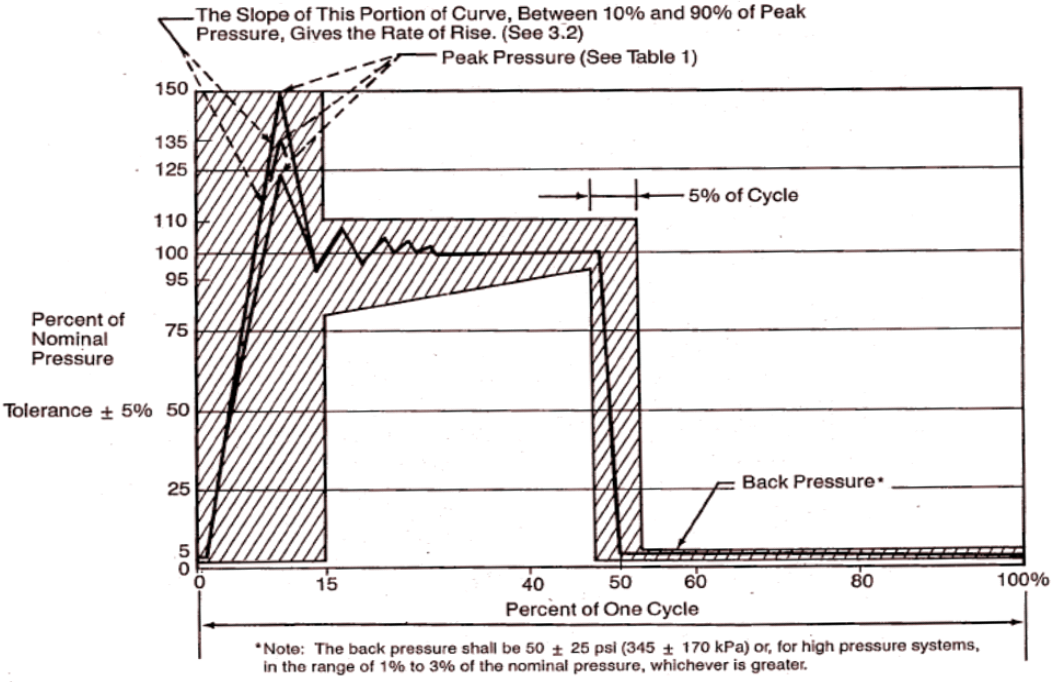

Figure 1. Impulse Trace

Figure 32, Fatigue loading

Table 13. Crack life prediction of 3/8" tubes compared with experiment

Specimen ID	a_o (in)	$2c_o$ (in)	Nominal pressure (psi)	Max. pressure (psi)	Exp.life (cycles)	Predicted Life
N212	0.009	0.036	4,500	6,300	90,300	90,600
N631	0.009	0.036	4,500	6,300	86,400	
N223	0.009	0.036	5,000	7,400	58,600	45,658
N623	0.009	0.036	5,000	7,400	50,100	
N132	0.009	0.036	5,500	8,250	36,250	28,798
N213	0.009	0.036	5,500	8,250	48,250	
N121	0.009	0.072	4,500	6,300	35,400	33,913
N122	0.009	0.072	4,500	6,300	44,725	
N511	0.009	0.072	5,000	7,500	22,000	16,169
N111	0.009	0.072	5,000	7,500	23,900	
N521	0.009	0.072	5,500	8,250	14,384	10,797
N531	0.009	0.072	5,500	8,250	14,384	

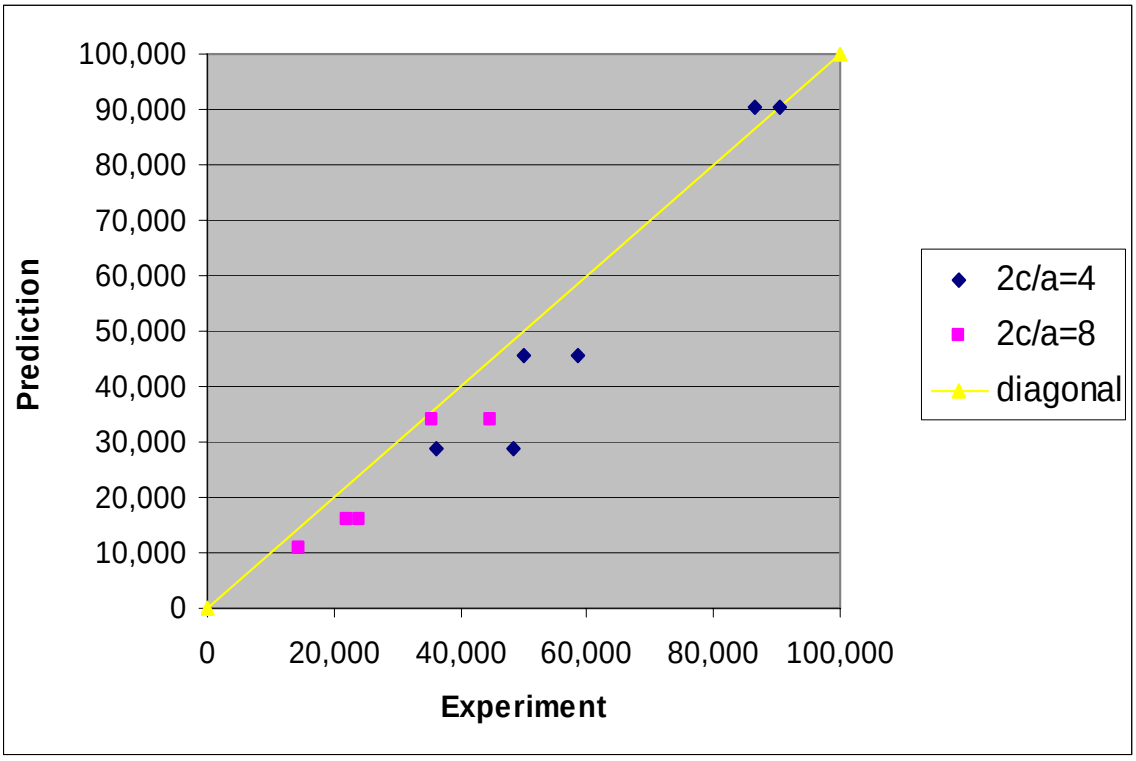

Figure 33, 3D FE modeling compared with experimental results

Table 14, Prediction and experimental life of 1/4” OD tubes

a, crack depth	2 mils	
2c, crack length	20 mils	50 mils
Experiment	> 200k	>200k
FE modeling	637,080	242,120

a, crack depth	4 mils	
2c, crack length	20 mils	50 mils
Experiment	> 200k	98,466 107,162
FE modeling	318,200	83,650

a, crack depth	6 mils	
2c, crack length	20 mils	50 mils
Experiment	> 200k	63,768 72,340
FE modeling	212,200	42,120

Table 15, Prediction and experimental life of 1/2” OD tubes

a, crack depth	2 mils	
2c, crack length	20 mils	50 mils
Experiment	n/a	>200k
FE modeling	n/a	333,450

a, crack depth	4 mils	
2c, crack length	20 mils	50 mils
Experiment	> 200k	135,879 149,134
FE modeling	456,940	162,620

a, crack depth	6 mils	
2c, crack length	20 mils	50 mils
Experiment	> 200k	107,057 109,117
FE modeling	326,730	101,440

Table 16, Prediction and experimental life of 5/8” OD tubes

a, crack depth	2 mils
2c, crack length	50 mils
Experiment	307,792 336210
FE modeling	380,430

a, crack depth	4 mils
2c, crack length	50 mils
Experiment	170,274 181,865
FE modeling	198,930

a, crack depth	6 mils
2c, crack length	50 mils
Experiment	132,102 137,337
FE modeling	129,470

Table 17, Prediction and experimental life of 3/4” OD tubes

a, crack depth	2 mils
2c, crack length	50 mils
Experiment	403,163 403,581
FE modeling	415,300

a, crack depth	4 mils
2c, crack length	50 mils
Experiment	167,876 168,114
FE modeling	227,430

a, crack depth	6 mils
2c, crack length	50 mils
Experiment	157,003 137,095
FE modeling	152,110

Table 18, Prediction and experimental life of 3/8" OD tubes

a, crack depth	2 mils	
2c, crack length	25 mils	50 mils
Experiment	>200k	>200k
FE modeling	485,500	267,720

a, crack depth	4 mils
2c, crack length	25 mils
Experiment	171,332
FE modeling	240,450

a, crack depth	5 mils		
2c, crack length	20 mils	25 mils	50 mils
Experiment	> 200k	129,803	127,786
FE modeling	264,400	194,820	103,050

a, crack depth	7 mils
2c, crack length	20 mils
Experiment	120,151
FE modeling	196,250

a, crack depth	9 mils	
2c, crack length	25 mils	50 mils
Experiment	46,890	36,358
FE modeling	112,710	34,390

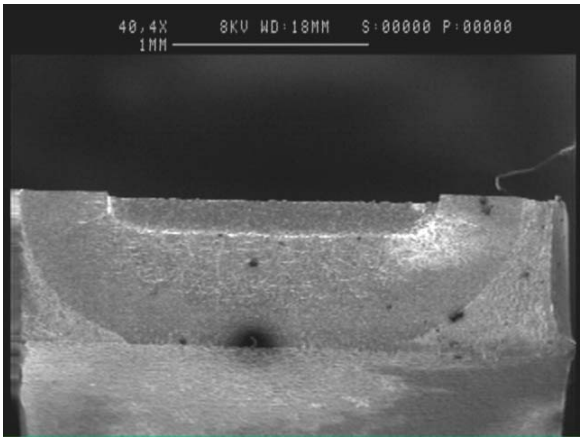

Figure 34.a, crack profile of medina size

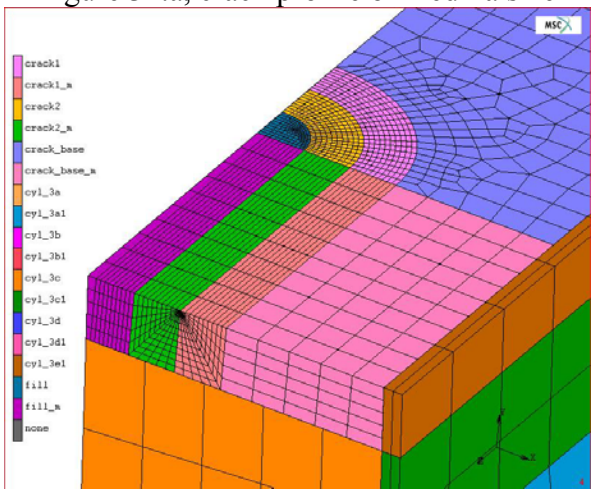

Figure 34.b, 3D FE modeling of medina size crack

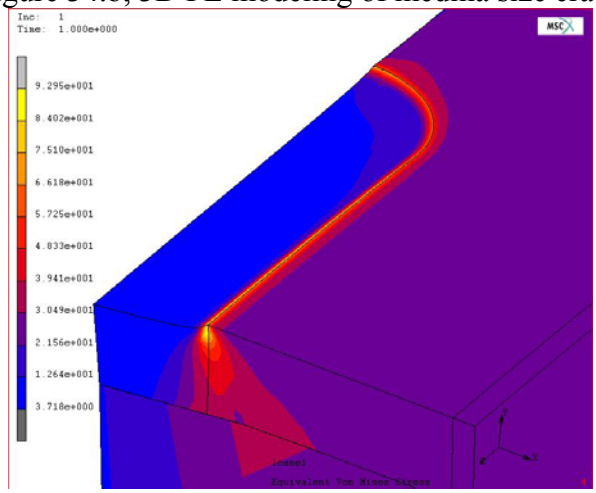

Figure 34.c, 3D FE stress result of medina size crack

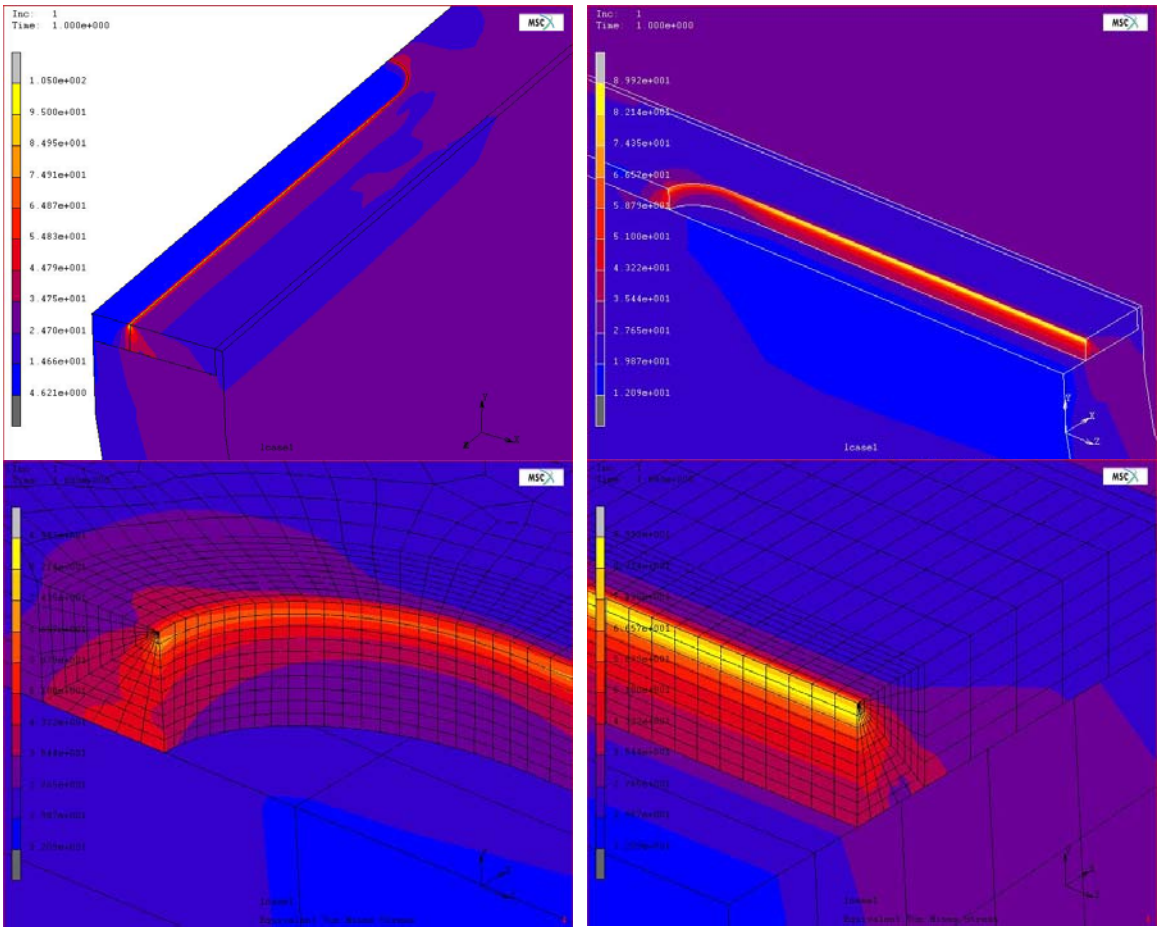

Figure 35, 3D FE modeling and stress distribution of very long cracks

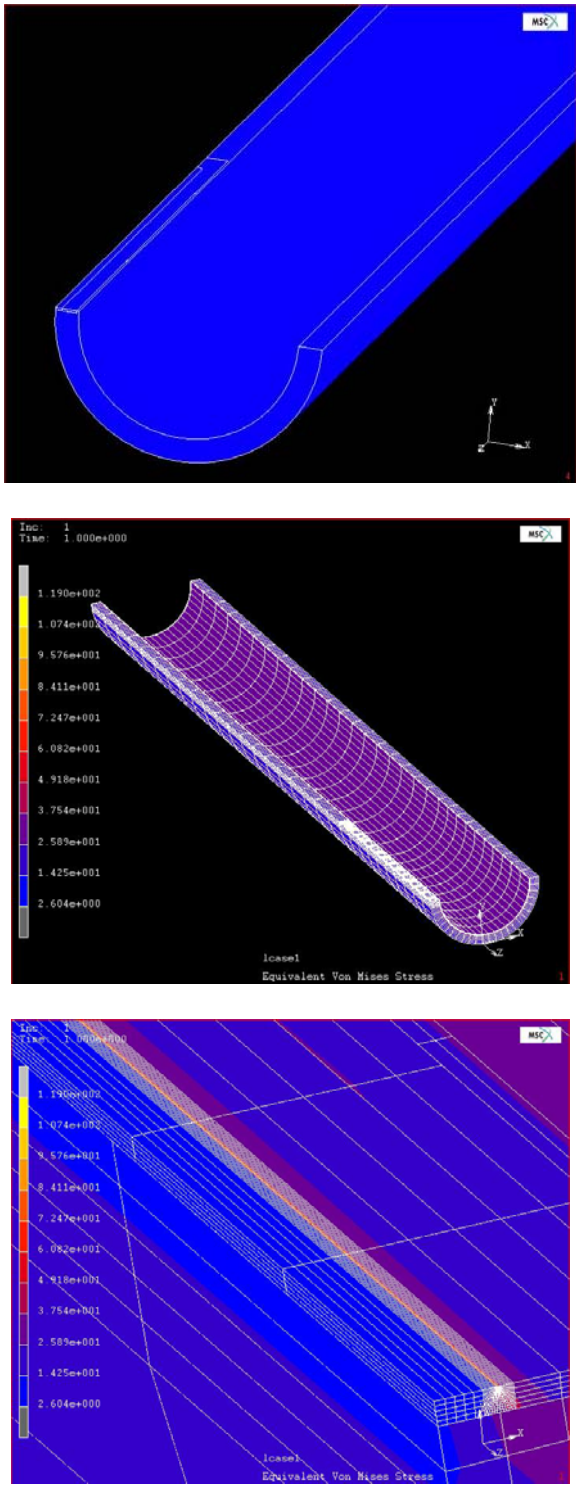

Figure 36, 3D FE modeling of very long crack in 1/4” tubes

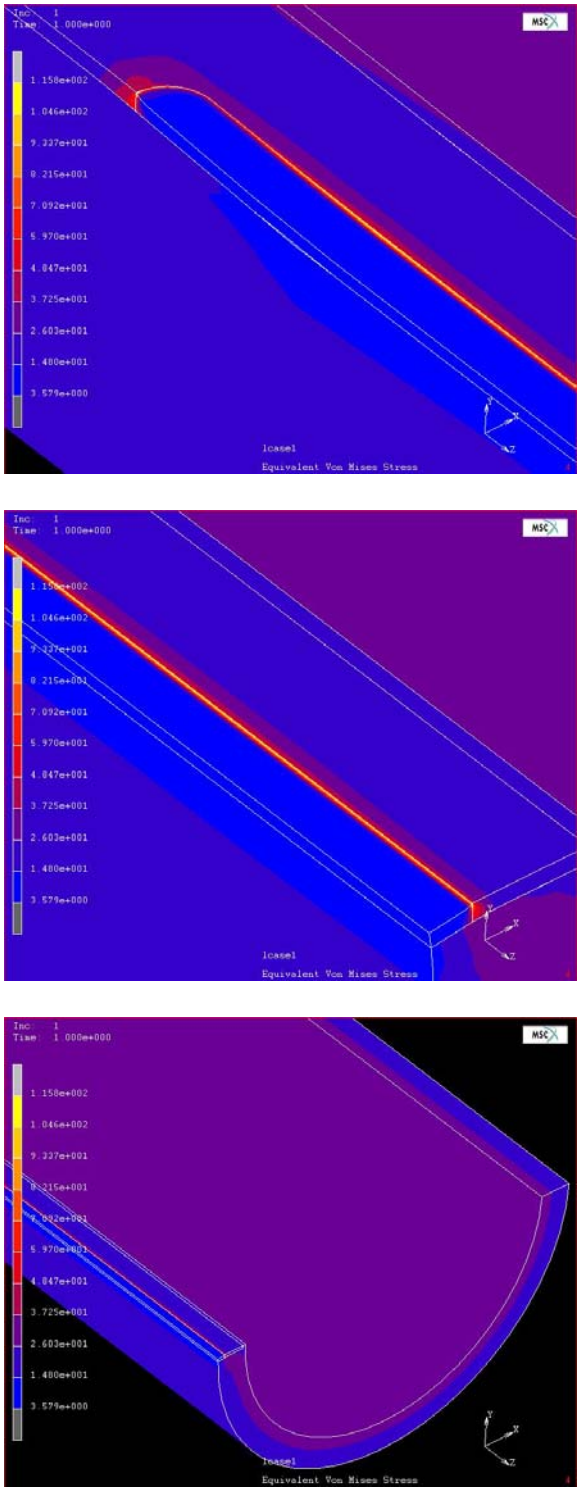

Figure 37, 3D FE modeling of very long crack in 1/2” tubes

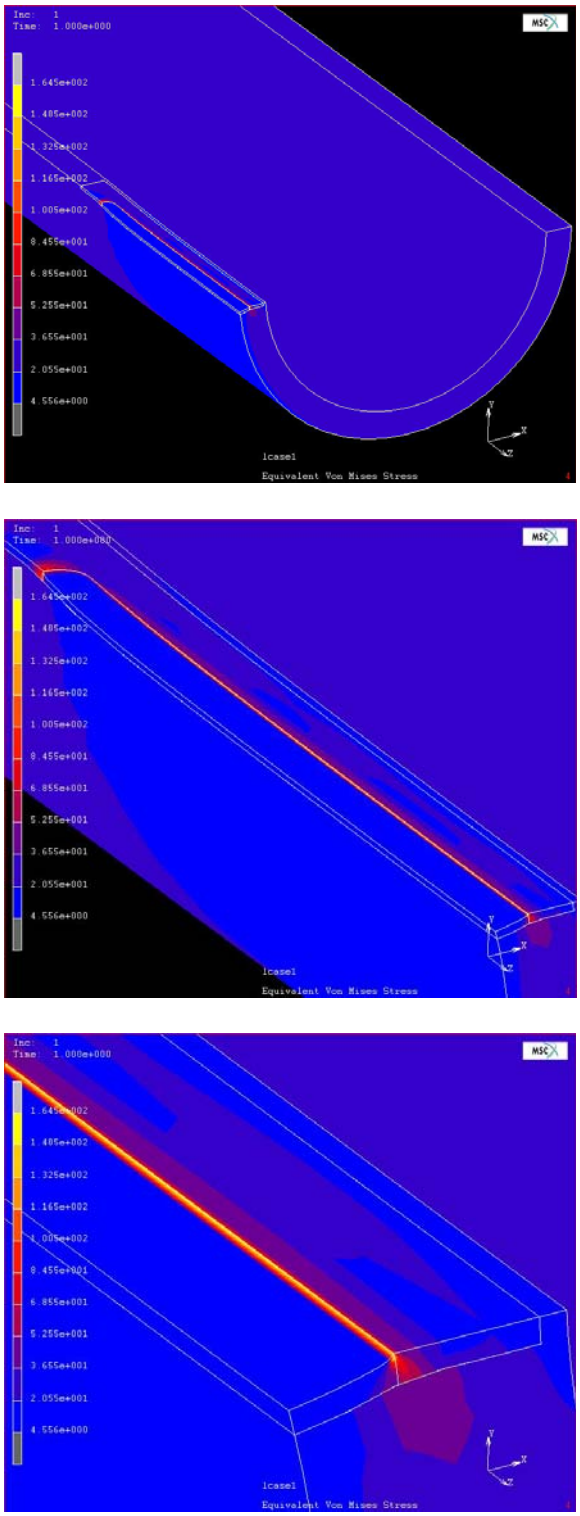

Figure 38, 3D FE modeling of very long crack in 5/8” tubes

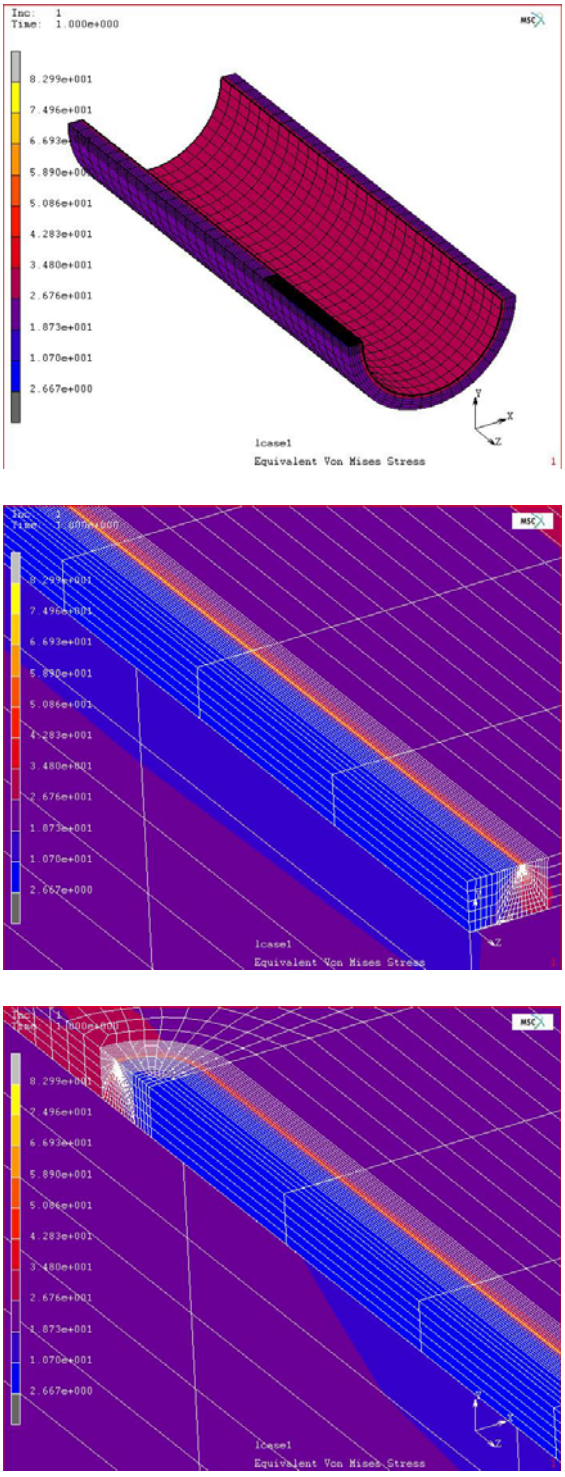

Figure 39, 3D FE modeling of very long crack in 3/4” tubes

Table 19, Prediction and experimental life of all tubes for the initial crack depth = 6 mils

1/4” tubes

a, crack depth	6 mils	
2c, crack length	0.5”	1”
Experiment	10,857 9,203	2,560 3,164
FE modeling	11,900	11,900

1/2” tubes

a, crack depth	6 mils	
2c, crack length	0.5”	1”
Experiment	29,557 27,400	22,668 31,068
FE modeling	34,415	34,415

5/8” tubes

a, crack depth	6 mils	
2c, crack length	0.5”	1”
Experiment	38,885 40,740	34,650 36,042
FE modeling	67,566	67,566

3/4” tubes

a, crack depth	6 mils	
2c, crack length	0.5”	1”
Experiment	50,223 50,667	53,716 54,774
FE modeling	76,103	76,103

Table 20, Prediction and experimental life of all tubes for the initial crack depth = 4 mils

1/4” tubes

a, crack depth	4 mils	
2c, crack length	0.5”	1”
Experiment	28,437 31,193	22,137 19,798
FE modeling	29,040	29,040

1/2” tubes

a, crack depth	4 mils	
2c, crack length	0.5”	1”
Experiment	35,371 36,194	29,307 42,370
FE modeling	22,194	22,194

5/8” tubes

a, crack depth	4 mils	
2c, crack length	0.5”	1”
Experiment	71,076 72,806	51,669 53.750
FE modeling	89,876	89,876

3/4” tubes

a, crack depth	4 mils	
2c, crack length	0.5”	1”
Experiment	92,287 83,172	66,504 43.377
FE modeling	105,698	105,698

Table 21, Prediction and experimental life of all tubes for the initial crack depth = 2 mils

1/4” tubes

a, crack depth	2 mils	
2c, crack length	0.5”	1”
Experiment	84,887 92,583	77,527 64,058
FE modeling	91,855	91,855

1/2” tubes

a, crack depth	2 mils	
2c, crack length	0.5”	1”
Experiment	136,553 136,933	126,344 299,083
FE modeling	101,584	101,584

5/8” tubes

a, crack depth	2 mils	
2c, crack length	0.5”	1”
Experiment	138,034 151,397	147,891 168,867
FE modeling	206,958	206,958

3/4” tubes

a, crack depth	2 mils	
2c, crack length	0.5”	1”
Experiment	215,954 242,444	144,086 137,298
FE modeling	237,548	237,548

Table 22, Prediction and experimental life of long cracks of 3/8” tubes

3/8” tubes

a, crack depth	2 mils	
2c, crack length	1”	1.5”
Experiment	182,412	172,365
FE modeling	203,477	203,477

3/8” tubes

a, crack depth	5 mils	
2c, crack length	1”	1.5”
Experiment	17,125	18,023
FE modeling	24,000	24,000

3/8” tubes

a, crack depth	9 mils	
2c, crack length	1”	1.5”
Experiment	2,300	1,860
FE modeling	3,410	3,410